



# DIGITAL ACCESS TO SCHOLARSHIP AT HARVARD

## The Molecular Characterization of the Mitochondrial Calcium Uniporter

The Harvard community has made this article openly available. [Please share](#) how this access benefits you. Your story matters.

<b>Citation</b>	No citation.
<b>Accessed</b>	February 16, 2015 1:22:27 PM EST
<b>Citable Link</b>	<a href="http://nrs.harvard.edu/urn-3:HUL.InstRepos:12407621">http://nrs.harvard.edu/urn-3:HUL.InstRepos:12407621</a>
<b>Terms of Use</b>	This article was downloaded from Harvard University's DASH repository, and is made available under the terms and conditions applicable to Other Posted Material, as set forth at <a href="http://nrs.harvard.edu/urn-3:HUL.InstRepos:dash.current.terms-of-use#LAA">http://nrs.harvard.edu/urn-3:HUL.InstRepos:dash.current.terms-of-use#LAA</a>

*(Article begins on next page)*

**MOLECULAR CHARACTERIZATION OF THE MITOCHONDRIAL CALCIUM  
UNIPORTER**

by

**Molly Plovanich**

**Submitted in Partial Fulfillment of the Requirements for the M.D. Degree  
with Honors in a Special Field**

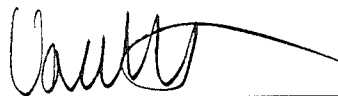
**February 3, 2014**

Area of Concentration: Cell Biology/Calcium/Ion Transport

Project Advisor: Vamsi K. Mootha, MD

Author's Prior Degrees: B.A. Biophysics

I have reviewed this thesis. It represents work done by the author under my supervision and guidance.



Faculty Sponsor's Signature

## Table of Contents

Glossary	3
Abstract	4
Introduction	6
Chapter 1	
Introduction	12
Materials and Methods	13
Results	18
Discussion	32
Chapter 2	
Introduction	35
Materials and Methods	37
Results	41
Discussion	56
Conclusion	60
Summary	62
References	64

## Glossary

MCU	Mitochondrial calcium uniporter
MICU1	Mitochondrial calcium uptake 1 (formerly EFHA3, CBARA1)
MICU2	Mitochondrial calcium uptake 2 (formerly EFHA1)
MICU3	Mitochondrial calcium uptake 3 (formerly EFHA2)
EMRE	Essential MCU regulator
IP	Immunoprecipitation
siRNA	Small interfering RNA
shRNA	Short hairpin RNA
SDS-PAGE	Sodium dodecyl sulfate polyacrylamide gel electrophoresis
BN-PAGE	Blue native polyacrylamide gel electrophoresis
PBS	Phosphate buffered saline
DMEM	Dulbecco's modified eagle medium
IVT	In vitro translation
EGTA	Ethylene glycol tetraacetic acid
CCCP	Carbonyl cyanide m-chlorophenyl hydrazone
TMRM	Tetramethyl rhodamine methyl ester
CG5N	Calcium Green-5N
ATP	Adenosine Triphosphate
Ru-360	Ruthenium 360

## **Abstract**

The mitochondrion is a double-membrane bound organelle present in all eukaryotes. The descendant of an ancient bacterial ancestor, it has evolved a vast number of roles in eukaryotes, including ATP production, fatty acid oxidation, steroid synthesis and apoptosis. Interestingly, mitochondria from a diverse set of organisms have the ability to transport large amounts of calcium, an essential signaling molecule in the eukaryotic cell. This represents an important gateway connecting mitochondrial function with the rest of the cell.

By buffering cytosolic calcium, mitochondria can shape the magnitude and duration of intracellular calcium transients, which in turn govern key physiological events, including neurotransmission, oscillatory hormone release and cell differentiation. Although controlled uptake of calcium into the matrix influences the rate of ATP production, excess calcium within the matrix triggers non-specific permeabilization of the mitochondrial inner membrane, resulting in cell death. Consequently, mitochondrial calcium transport is thought to be essential in mediating life and death decisions in the eukaryotic cell.

Despite its importance in cellular physiology, the molecular identity of the mitochondrial calcium uniporter remained a mystery for nearly five decades. Recently, an approach inspired by comparative genomics was used to identify two proteins required for high-capacity mitochondrial calcium uptake. These include MICU1, an EF-hand protein that may function as a regulatory component by sensing calcium, and MCU, the channel-forming subunit of the uniporter. Moving forward, it will be important to elucidate how these proteins function in concert to achieve high-capacity mitochondrial calcium uptake.

In this work, I explore two distinct areas within the growing field of molecular mitochondrial calcium biology. First, I discuss the identification of a new protein, MICU1-paralog EFHA1, and present data that implicates it in mitochondrial calcium uptake. Subsequently, I describe efforts to establish an *in vitro* system to characterize the channel activity of MCU, including my contribution to the development of a liposome-based assay for calcium transport and preliminary work aimed at reconstituting MCU transport activity in proteoliposomes.

Impaired mitochondrial calcium transport has been linked to the pathogenesis of cancer, neurodegeneration and ischemic injury. The therapeutic potential of targeting this pathway is promising, but further experiments are needed to clarify the role of mitochondrial calcium transport in cellular physiology and disease. The molecular characterization of the uniporter offers a diverse set of genetic approaches to tackle this question and opens the possibility of targeting components of the uniporter in human disease.

## Introduction

The mitochondrion is a double-membrane bound organelle located in the cytosol of all nucleated eukaryotic cells. Derived from an  $\alpha$ -proteobacteria ancestor<sup>1</sup>, the mitochondrion is a fundamental component of the modern eukaryotic organism. Although the mitochondrion retains a distinct genome encoding 13 proteins on a single, circular chromosome, the vast majority of mitochondrial proteins are encoded in the nuclear genome<sup>2</sup>, which highlights the extensive integration of this unique organelle into the eukaryotic cell.

Throughout evolution, the mitochondrion has emerged as the primary site of ATP production, which is essential for ion homeostasis, metabolic regulation and cellular division. Within mitochondria, numerous enzymes work in concert to facilitate oxidative phosphorylation. This process involves coupling the oxidation of high-energy electron donors to the generation of a proton gradient across the mitochondrial inner membrane, which in turn drives ATP production via ATP synthase<sup>3</sup>. In addition to generating cellular energy, mitochondria have essential roles in a diverse set of cellular processes, including fatty acid oxidation, heme synthesis, steroid synthesis and apoptosis<sup>4-7</sup>.

An important gateway that connects mitochondria with the cell is mitochondrial calcium uptake. The capacity of mitochondria to buffer cytosolic calcium enables mitochondria to shape the magnitude and duration of intracellular calcium transients, which in turn govern key physiological events, including neurotransmission, oscillatory hormone release and cell differentiation<sup>8-10</sup>. Within the mitochondrial matrix, calcium activates several dehydrogenases that produce high-energy electron donors that are substrates for oxidative phosphorylation<sup>11</sup>. This regulatory mechanism enables mitochondrial calcium uptake to alter oxidative metabolism<sup>12</sup>. Although controlled uptake

of calcium into the matrix influences the rate of ATP production, excess calcium within the matrix triggers non-specific permeabilization of the mitochondrial inner membrane, resulting in cell death<sup>7,13</sup>. Therefore, mitochondrial calcium uptake is an important regulatory point that enables mitochondria to coordinate a diverse set of cellular events with ATP production.

The phenomenon of mitochondrial calcium uptake was discovered over 50 years ago in isolated rat mitochondria<sup>14,15</sup>. These landmark experiments showed that isolated mitochondria have the capacity to take up large amounts of calcium present in the buffer. Follow up studies revealed that this transport activity was present in mitochondria isolated from a diverse set of organisms, including chicken, turtle and *Neurospora crassa*<sup>16</sup>. The biophysical properties of this high-capacity uptake mechanism were described extensively in subsequent work. These experiments demonstrated that the uptake mechanism was dependent on mitochondrial membrane potential, allosterically activated by calcium and sensitive to ruthenium red<sup>15,17,18</sup>. Furthermore, mitochondrial calcium uptake was not coupled to another ion, thereby establishing it as a high-capacity uniporter mechanism<sup>19,20</sup>. These findings were extended to intact cells following the development of genetically encoded calcium indicators that could be targeted to the mitochondria<sup>21</sup>. Patch clamp studies further corroborated these findings by providing evidence that the uniporter mechanism is due to a highly selective ion channel<sup>22</sup>. Despite its central importance in cellular physiology, the molecular identity of the mitochondrial calcium uniporter remained a mystery for nearly five decades, eluding attempts to purify it from mitochondria isolated from a wide array of animal tissues<sup>23,24</sup>.



Recently, the Mootha lab pioneered a novel approach to identify components of the mitochondrial calcium uniporter<sup>25,26</sup>. The observation that uniporter activity is present in vertebrates and kinetoplastids, yet absent in *Saccharomyces cerevisiae* motivated a computational strategy to prioritize genes that match this evolutionary profile and localize to the mitochondria. These criteria generated a list of 58 candidate genes. When a subset of these candidates were screened using a loss-of-function cell-based assay, *MICU1*, a poorly studied gene containing EF-hands, was identified as a putative regulatory subunit of the mitochondrial calcium uniporter<sup>25</sup>. In a follow-up study, *MICU1* was used as “computational bait” to identify genes with a similar evolutionary signature and expression pattern across different tissues. This led to the discovery of a novel transmembrane protein, named MCU, which encodes the elusive pore-forming subunit of the mitochondrial calcium uniporter<sup>26</sup>.

In this thesis, I present two bodies of work, each which explores a distinct area within the growing field of molecular mitochondrial calcium biology. First, I discuss the identification of a new gene, *MICU1*-paralog *EFHA1*, now called *MICU2*, and present data that implicates this protein in mitochondrial calcium uptake. Secondly, I discuss my contribution to establishing a system to characterize the channel activity of MCU, including the development of a liposome transport assay for calcium, and preliminary work in proteoliposome reconstitution of MCU.

Since completion of this work, a number of important studies have been published which shed light on how MCU, *MICU1* and *MICU2* interact to coordinate high capacity mitochondrial calcium transport. In the initial characterization of *MICU1*, there was a striking defect in the rise of mitochondrial free calcium in response to agonist stimulation<sup>25</sup>, suggesting that calcium conductance via the uniporter was decreased,

though reduced uniporter conductance was not formally demonstrated. This profound defect was also observed in cells expressing exogenous MICU1 with mutated EF-hands on a knockdown background, pointing to the critical function of MICU1's EF-hands in mediating high-capacity mitochondrial calcium uptake. At this time, it was postulated that MICU1 likely functions as either 1) a calcium buffer with a secondary impact on calcium transport or 2) a calcium sensor that directly interacts with a channel protein to impart allosteric regulation of calcium transport across the inner mitochondrial membrane<sup>25</sup>. Since this discovery, a number of studies have clarified that MICU1 in fact has two critical roles in regulating mitochondrial calcium transport. First, it acts as a gatekeeper to keep MCU closed at low cytosolic calcium concentrations (<500 nM)<sup>27-29</sup>, and secondly, it imparts cooperativity to MCU via its EF-hands, thereby enabling high capacity uptake in response to abrupt rises in cytosolic calcium<sup>27,29</sup>. Although there has been controversy in whether MICU1 imparts cooperativity to MCU transport, multiple studies have confirmed that MICU1 is indeed a co-factor necessary for cooperative calcium uptake at high calcium concentrations<sup>27,29</sup>. The discrepancy in whether MICU1 imparts cooperativity to MCU transport likely stems from the absence of physiological magnesium in the transport assay used by Mallilankaraman et al. given that magnesium has previously been shown to be a necessary co-factor for allosteric regulation of the uniporter. In light of these new studies, the significantly blunted rise in free mitochondrial matrix calcium in response to agonist stimulation in MICU1 knockdown cells was likely due to a combination of reduced MCU expression, altered matrix buffering and altered matrix pH rather than a dramatic decrease in calcium conductance.

In addition to a deeper understanding of MICU1, recent studies have confirmed that MCU is indeed the pore-forming subunit that enables calcium transport across the

mitochondrial inner membrane. Perhaps, the most definitive evidence in support of this function is data from voltage-clamping mitoplasts (vesicles composed of inner mitochondrial membrane) measuring uniporter current in the setting of altered MCU expression<sup>30</sup>. These experiments unequivocally demonstrated that knockdown of MCU abrogates uniporter current, overexpression of MCU increases current and that a point mutation in the pore domain abolishes sensitivity to Ruthenium 360, the most specific inhibitor of uniporter current. Interestingly, *MCU* has a paralog which has been named *MCUb* (CCDC109b) that has ~50% sequence similarity to MCU<sup>31</sup>. Of note, the protein sequence harbors mutations in the predicted pore domain and exerts a dominant negative effect in cell culture and planar lipid bilayer experiments, which may represent an additional mechanism of control over mitochondrial calcium transport.

Within the past few months, an additional component of the uniporter complex was identified using mass spectrometry. This protein, EMRE, is required for uniporter channel activity<sup>32</sup>. In addition, it is required for the interaction between MCU and MICU1, suggesting that it bridges the calcium-sensing role of MICU1 with the channel activity of MCU. In this study and others, MICU1 and MICU2 are within the intermembrane space, though this remains a subject of ongoing debate<sup>32</sup>. At present, the current data points to a model in which MCU forms a high capacity calcium channel that is inhibited under low calcium concentrations by MICU1 and MICU2, which release their inhibitory effects at higher calcium concentration via calcium binding to their EF-hands.

Several studies have implicated mitochondrial calcium uptake in the pathogenesis of cancer, neurodegeneration and ischemic injury<sup>7,33-36</sup>. A recent study reports the first mutation in *MICU1* in an individual with progressive myopathy, learning difficulties and a progressive extrapyramidal movement disorder, underscoring the

importance of mitochondrial calcium handling in human disease<sup>37</sup>. Much like the results in cell culture, fibroblasts isolated from this individual demonstrated increased calcium transport at low cytosolic calcium concentrations in the setting of mutated MICU1, further solidifying the role of MICU1 as a negative regulator of uniporter activity at low calcium concentrations<sup>37</sup>. In a study describing the first *MCU* knockout mouse, there was impaired activity of pyruvate dehydrogenase, a mitochondrial calcium-activated enzyme, in skeletal muscle in mice lacking MCU expression<sup>38</sup>. The most striking phenotype in this study was the impaired ability of MCU null mice to perform strenuous work. Despite the exciting therapeutic potential raised by these findings, the role of mitochondrial calcium transport in cellular physiology and disease has yet to be fully explored. The molecular characterization of the uniporter and its regulators represents a major advance towards this goal and opens up the possibility of targeting components of the uniporter for the treatment or prevention of disease.

## Chapter 1: MICU2 is a paralog of MICU1 that partners with the uniporter to control mitochondrial calcium uptake

### INTRODUCTION

Recently, a novel approach coupling insights from comparative physiology and integrative genomics led to the identification of two proteins required for high-capacity mitochondrial calcium uptake, which include MICU1<sup>25</sup> and MCU<sup>26</sup>. Based on sequence analysis and functional studies, we hypothesized that MCU is the channel-forming subunit of the uniporter, whereas MICU1 is a key regulatory component that senses calcium via its EF hands. This model has been corroborated by independent and complementary studies<sup>39</sup> which suggest that MICU1 inhibits MCU at resting cytosolic calcium concentrations and triggers allosteric activation of the channel at high cytosolic concentrations.

Interestingly, genome sequence analysis reveals that MICU1 has two human homologs, *EFHA1* and *EFHA2*, neither of which has been studied. Both of these proteins have mitochondrial targeting sequences and were previously identified with high and low confidence, respectively, in MitoCarta, a proteomic characterization of mitochondria from 14 different mouse tissues<sup>2</sup>. In this work, we sought to determine whether *EFHA1* is also critical for mitochondrial calcium uptake. Decades of research have shown that uniporter activity exists in all vertebrate tissues, but that its regulation is distinct<sup>16,40</sup>. It is possible that the presence of multiple regulatory proteins could provide a molecular explanation for tissue specific regulation of the mitochondrial calcium uniporter.

## **MATERIALS AND METHODS**

### *Multiple sequence alignment*

Sequences were downloaded from the NCBI protein database. ClustalW2 was used to multiple sequence alignment and generate a phylogenetic tree.

### *Cell Culture*

HeLa and HEK293T cells were received from the ATCC. HeLa cells expressing aequorin targeted to the mitochondrial matrix (mt-AEQ) were purchased from Aequotech (AT-002-H). Cells were grown at 37°C and 5% CO<sub>2</sub> in Dulbecco's modified Eagle medium (DMEM) (Invitrogen 11995) with 10% FBS (Sigma F6178). HeLa cells expressing mt-AEQ were cultured in 100 µg/ml of geneticin.

### *Confocal imaging*

HeLa cells were transfected with plasmids containing carboxy terminus GFP-tagged MICU2 or Mito-HcRed1 (Clontech 632434). Twenty-four hours after transfection, cells were washed three times with PBS, then imaged using a Leica TCS SP5 confocal microscope.

### *Immunoprecipitation*

Mitochondria were isolated from HEK-293T cells that stably express Flag-tagged GFP targeted to mitochondria or MCU-Flag. 200 µg of protein were solubilized using 200 µl of lysis buffer (50 mM HEPES pH 7.4, 150 mM NaCl, 5 mM EDTA, 0.2% DDM and protease inhibitor tablets (Roche Applied Science 118361170001)) for 10 minutes at 4 °C. Lysates were cleared by spinning at 16000g for 10 minutes at 4 °C. Cleared lysates

were incubated with 10  $\mu$ l of anti-Flag M2 affinity gel (Sigma A2220) in PBS for 2 hours at 4 °C. Immunoprecipitates were washed with 1 ml of lysis buffer 3 times, and boiled in 30  $\mu$ l of sample buffer. A third of the immunoprecipitate was loaded on a 12% SDS-PAGE gel for detection of the indicated proteins. MCU antibody was generated in chicken, MICU1 antibody was generated in rabbit and MICU2 antibody was purchased from Abcam (ab101465).

#### *Synthesis and selection of siRNA duplexes targeting MICU1 and MICU2*

48 and 20 siRNAs were selected for synthesis and screening based on low-predicted off-target potentials and 100% homology with mouse sequences NM\_144822.2 and NM\_028643.3, respectively. Single-strand RNAs were produced at Alnylam Pharmaceuticals as previously described<sup>41</sup>. Hepa-1c1c7 cells seeded at 15,000 cells per well in 96-well plates were transfected with siRNAs using Lipofectamine RNAiMAX according to the manufacturer's protocols. Each experiment was performed in technical duplicate. 18-24h post-transfection, *MICU1* and *MICU2* mRNA levels were quantified using a branched-DNA assay (QuantiGene Reagent System, Panomics) according to the manufacturer's protocols. Their mRNA levels were normalized to GAPDH mRNA.

#### *In vivo silencing of MICU1 and MICU2*

All procedures used in animal studies were approved by the Institutional Animal Care and Use Committee. C57BL/6 mice (Charles River Laboratories) received either PBS or siRNA in lipidoid formulations via weekly tail vein injections as previously described<sup>26,42-44</sup>. After overnight fasting, the animals were euthanized by CO<sub>2</sub> inhalation and the livers

were harvested and stored in ice-cold PBS prior to mitochondria isolation. A piece of liver tissue was snap-frozen in liquid nitrogen for mRNA analysis.

#### *Mitochondrial Isolation*

Mitochondria were isolated from mouse liver as previously described<sup>45</sup> and resuspended in a buffer containing 220 mM mannitol, 75 mM sucrose, 10 mM HEPES and 1 mM EDTA, adjusted to pH 7.4 with KOH, and supplemented with fresh 0.2% BSA prior to use. Mitochondria were stored on ice until further use.

#### *Measurement of mitochondrial respiration and membrane potential in isolated mitochondria*

Respiration and membrane potential were measured optically as previously described<sup>45</sup>. Values for respiratory control ratios (RCR) and ADP:O (P:O) ratios represent the mean +/- s.d. of three independent experiments performed on n=3 mice.

#### *Measurement of mitochondrial calcium uptake in isolated mitochondria*

Calcium uptake was performed on a Perkin-Elmer Envision plate reader and Perkin Elmer LS-50B fluorescence spectrometer as previously described<sup>26</sup>. Inset reports linear fits between 5 and 10s from experiments performed on n=3 mice.

#### *RNA interference*

To silence *MICU1*, we used short-hairpin RNA (shRNA) constructs (TRCN0000053370, 5'-GCAATGGCGAACTGAGCAATA-3', sh-*MICU1*<sub>a</sub> and TRCN0000053368, 5'-GCAGCTCAAGAAGCACTTCAA-3', sh-*MICU1*<sub>b</sub>) from the Broad Institute's RNAi



Consortium (TRC) previously validated in mt-AEQ HeLa cells. As controls, shRNAs targeting *GFP*, *RFP* and *LACZ* were used. All shRNAs were provided in a lentiviral vector (pLKO.1) through the TRC. Lentiviral production and infection was performed as previously described<sup>46</sup>. Cells were selected 24 hours after infection with 2 mg/ml of puromycin.

#### *cDNA rescue experiments*

A lentiviral vector (pLEX983) for expressing C-terminal V5-tagged cDNA was obtained from the TRC. Full-length *MICU2* cDNA was synthesized (Blue Heron Biotechnology) and cloned into pLEX983. Lentivirus was produced using cDNAs encoding *GFP*, *MICU2* or *MICU1* resistant to TRCN0000053370 as previously described<sup>46</sup>. Virus was used to infect HeLa cells stably expressing mt-AEQ. Cells were selected 24 hours after infection with 5 µg/ml of blasticidin.

#### *Measurement of mitochondrial calcium in HeLa cells expressing mt-AEQ*

40,000 cells were seeded in a 96-well plate, incubated overnight with mitochondrial calcium measured following histamine treatment as previously described<sup>47</sup>. Light emission was measured at 469 nm every 0.1s using a luminometer (MicroBeta<sup>2</sup> LumiJET Microplate Counter PerkinElmer). Subsequently, luminescence was normalized to account for cell number.

#### *Blue native PAGE studies*

5 µg of mitochondria isolated from mouse liver or HeLa cells were solubilized in 2% digitonin on ice for 30 minutes. Electrophoresis was performed using the Novex

NativePAGE Bis-Tris Gel System from Invitrogen. Western blot analysis was performed using an MCU antibody generated in chicken. A commercially available antibody to ATP5A1 (MitoSciences MS507) was used as a loading control.

## RESULTS

### *MICU1, MICU2, and MICU3 form a family of paralogs*

In previous work, we used comparative genomics to identify *MICU1*, a mitochondrial protein essential for normal mitochondrial calcium handling in HeLa cells<sup>25</sup>. *MICU1*, previously known as *CBARA1* or as *EFHA3*, has a mitochondrial targeting sequence as well as two evolutionarily conserved EF hands. Genome sequence analysis reveals that *MICU1* shares significant sequence similarity with two human genes, *EFHA1* and *EFHA2*, neither of which has been studied before. These three proteins are conserved in vertebrates, whereas only one homolog is present in plants and protozoa.

I performed a multiple sequence alignment using homologs from vertebrates, plants and protozoa which placed the protozoa and plant homologs as outgroups on a phylogenetic tree (Figure 1a), thereby indicating that *EFHA1* and *EFHA2* are vertebrate paralogs of *MICU1* that likely arose from a gene duplication event prior to vertebrate evolution. Based on this finding, we have re-named *EFHA1* as *MICU2*, and *EFHA2* as *MICU3*.

*MICU2* and *MICU3* have N-terminal targeting sequences consistent with mitochondrial localization, much like *MICU1* (22). In our previous proteomic studies, *MICU2* and *MICU3* were detected in mitochondria from various mouse tissues, although their expression patterns differed significantly (16). *MICU1* was broadly expressed and detected in 12 out of 14 mouse tissues, whereas *MICU2* was detected in 7 out of 14 tissues with strong expression in visceral organs. In contrast, *MICU3* was found in 6 out of 14 tissues with a strong signature in skeletal muscle and the central nervous system. Despite being detected in multiple mouse tissues, *MICU3* lacked other evidence of

being mitochondrial, scoring just below the stringent threshold required to be a part of the MitoCarta collection. This is in contrast to MICU2, which was reported in MitoCarta and localized to the mitochondria using high-content microscopy.

Due to stronger evidence for mitochondrial localization and greater expression in visceral organs in which we can apply siRNA technology to achieve *in vivo* silencing, we decided to focus on *MICU2* for functional studies. Sequence comparison of human *MICU1* and *MICU2* reveals highly conserved domain architecture (Figure 1b). Similar to *MICU1*, *MICU2* has two EF-hands separated by a long stretch of residues predicted to form a helix. In previous work, we showed that the calcium-coordinating residues in the EF-hands of *MICU1* are highly conserved across species<sup>25</sup>. Like *MICU1*, *MICU2* demonstrates perfect conservation in the acidic residues that cap the EF-hands across evolution (Figure 1b).

#### *MICU2 localizes exclusively to mitochondria*

First, we confirmed that MICU2 localizes exclusively to mitochondria with confocal microscopy, which showed that a carboxy terminus GFP-tagged MICU2 overlapped with mitochondrial marker Mito-HcRed1 (Fig. 1c).

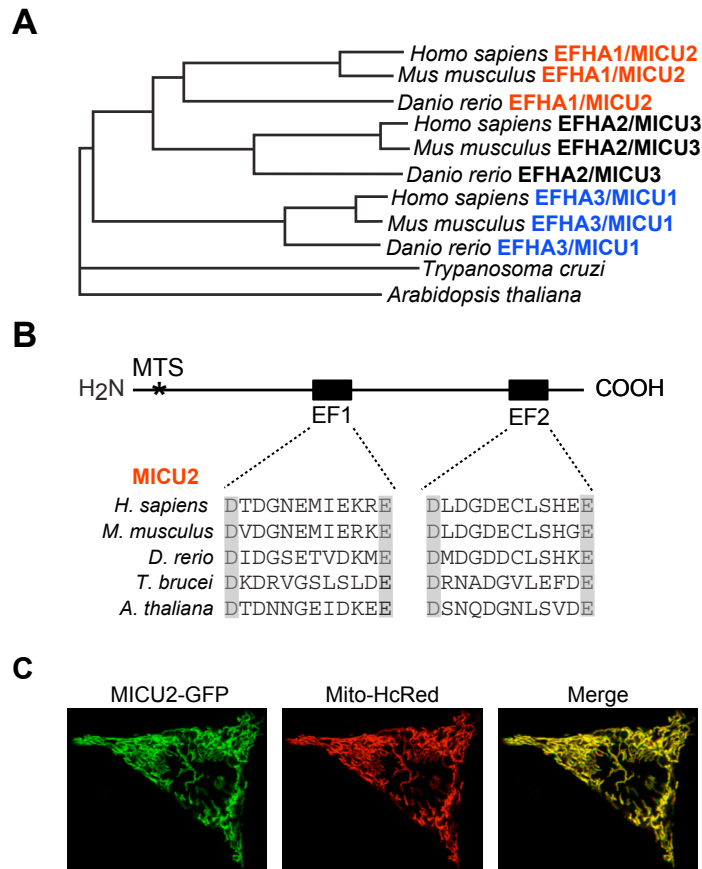


**Figure 1. *MICU2* is paralogous to *MICU1* and localizes exclusively to the mitochondrion. (a) *MICU1*, *MICU2* and *MICU3* share a common ancestor and are present in multiple vertebrate species. (b) *MICU2* has two evolutionarily conserved EF hands. (c) Representative confocal image of HeLa cells co-transfected with *MICU2*-GFP and Mito-HcRed1.**

### *MICU1* and *MICU2* are Cross-Stabilized at a Protein Level

Previously, we demonstrated that *MICU1* is required for normal mitochondrial calcium handling in HeLa cells. Given that *MICU1* and 2 are paralogs with conserved domain architecture, they may have redundant roles and be expressed in a mutually exclusive manner across different cell types. To address this possibility, we blotted whole cell lysate from HeLa cells for *MICU1* and *MICU2*, which demonstrated expression of both proteins (Figure 2a). Interestingly, in the setting of *MICU1* knockdown, there was a significant reduction in *MICU2* expression, suggesting that

these paralogs undergo cross-stabilization at a protein level (Figure 2a). This was observed following treatment with multiple hairpins that specifically target MICU1 and not MICU2 (sh-*MICU1<sub>a</sub>* and sh-*MICU1<sub>b</sub>*), indicating that this is a biological consequence of MICU1 loss rather than an off target effect.

#### *MICU2 associates with the MICU1/MCU complex*

To determine whether MICU2 physically interacts with these proteins, we performed immunoprecipitation on cells stably expressing either MCU-FLAG or GFP-FLAG. Although endogenous MICU1 and MICU2 were present in cell lysate from both cell lines, immunoprecipitation with an anti-FLAG antibody specifically recovered MICU1 and MICU2 from the MCU-FLAG cell line (Figure 2b). It is notable that the heterologous expression of MCU-FLAG resulted in increased protein expression of both MICU1 and MICU2, as seen in whole cell lysate (Figure 2b), suggesting that MCU overexpression either induces or stabilizes the expression of MICU1 and MICU2. Collectively, these results demonstrate that MICU2 physically interacts with MICU1 and MCU, further supporting a possible role for MICU2 in mitochondrial calcium uptake.

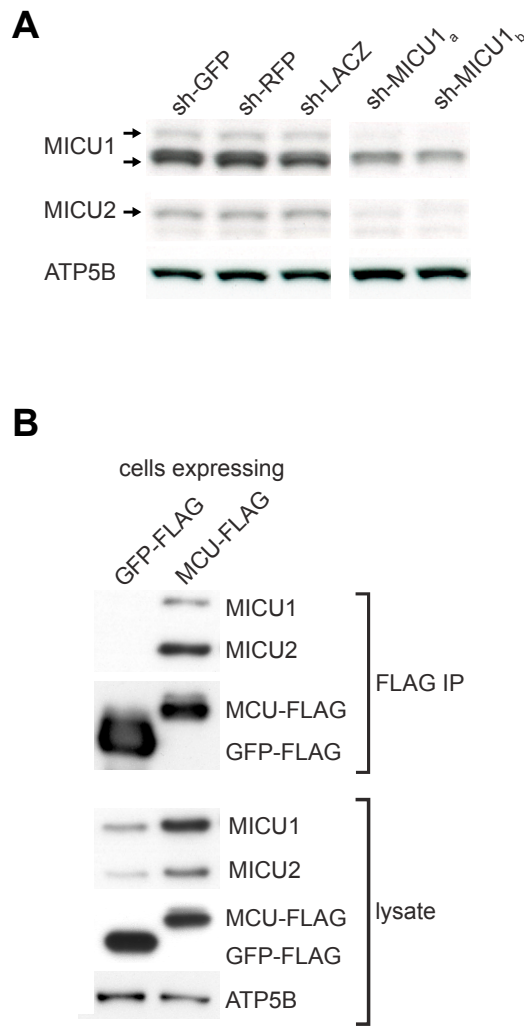


**Figure 2. MICU2 protein expression is stabilized by MICU1 and interacts with MCU and MICU1.** (a) Whole cell lysates from HeLa cells stably expressing a control sh-RNA (sh-GFP, sh-RFP, sh-LACZ) or a sh-RNA targeting *MICU1* (sh-MICU1a and sh-MICU1b) were blotted with anti-MICU1, anti-MICU2 and control anti-ATP5A. (b) Mitochondria isolated from HEK293T cells stably expressing MCU-FLAG or GFP-Flag targeted to mitochondria were solubilized with 0.2% DDM and subjected to anti-FLAG immunoprecipitation. Immunoprecipitates and lysate were blotted with anti-FLAG, anti-MICU1, anti-MICU2 and control anti-ATP5A.

*MICU1 and MICU2 can be silenced in vivo in mouse liver using siRNA technology*

Together, our sequence analysis and biochemical data motivated us to pursue studies in which we could directly assess the contribution of MICU2 to mitochondrial calcium uptake. To evaluate the impact of MICU2 loss on mitochondrial calcium uptake, we performed *in vivo* silencing of MICU2 in mouse liver using technology developed by

Alnylam Pharmaceuticals. We previously used this technology to report the first *in vivo* silencing of the uniporter<sup>26</sup>.

A key question was whether MICU1 and MICU2 contribute independently to mitochondrial calcium uptake. Therefore, we worked with collaborators at Alnylam to perform *in vivo* silencing of MICU1 in isolation and in combination with MICU2. We screened siRNA duplexes for both genes using previously described siRNA design and delivery technology<sup>26</sup>. Duplexes were transfected at concentrations from 1.25 to 5 nM, and the 3 siRNAs conferring the best knockdown were tested at different concentrations in the range of 7 pM to 5 nM to estimate their EC<sub>50</sub> in a mouse liver cell line (Figure 3a). As a negative control, we used a siRNA duplex that targets firefly luciferase (si-LUC). We performed a large-scale synthesis of one siRNA duplex and encapsulated it into a lipid-based formulation optimized for liver-specific delivery. Although mRNA knockdown was achieved at 24 hours, weekly tail vein injections of the siRNA duplexes were carried out over a six-week period to achieve *in vivo* protein knockdown of MICU1 and MICU2 (Figure 3b). Similar to *in vivo* silencing of MCU, mice did not exhibit any signs of distress, their weight was stable, and the gross appearance of their livers did not differ.



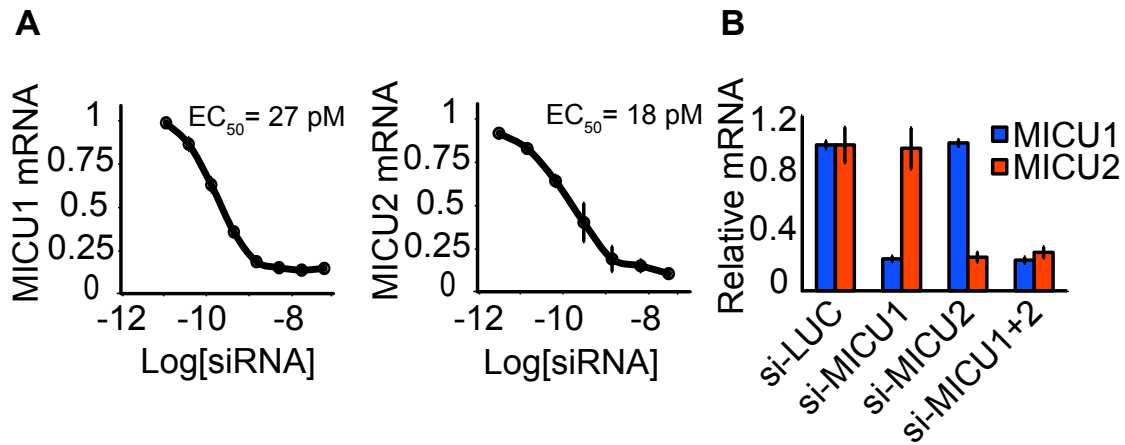


**Figure 3. *MICU1* and *MICU2* can be silenced *in vivo* in mouse liver using siRNA technology.** (a) *In vitro* dose-response curves of selected duplexes targeting *MICU1* and *MICU2*. (b) Relative expression of *MICU1* and *MICU2* mRNA after 6 weekly injections normalized to si-LUC mice.

*Mitochondrial membrane potential and respiration are intact following in vivo silencing of MICU1/MICU2 in mouse liver*

To begin, I evaluated the impact of silencing *MICU1* and *MICU2* on mitochondrial respiration and membrane potential ( $\psi_m$ ) to ensure that silencing did not cause respiratory chain collapse leading to a secondary defect in calcium uptake. Mitochondria isolated from control and knockdown livers underwent robust respiratory transitions as demonstrated by their comparable respiratory control ratios (RCR) (Figure 4a). In addition, comparable ADP:O ratios indicate intact ATP-coupled mitochondrial respiration. Together, these results indicate that silencing *MICU1* or *MICU2* did not alter mitochondrial respiration or oxidative phosphorylation. In mitochondria isolated from all treatment groups, membrane potential was responsive to ADP and fully depolarized by the uncoupler carbonyl cyanide m-chlorophenyl hydrazone (CCCP), indicating that silencing *MICU1* or *MICU2* did not adversely affect mitochondrial membrane potential (Figure 4b).

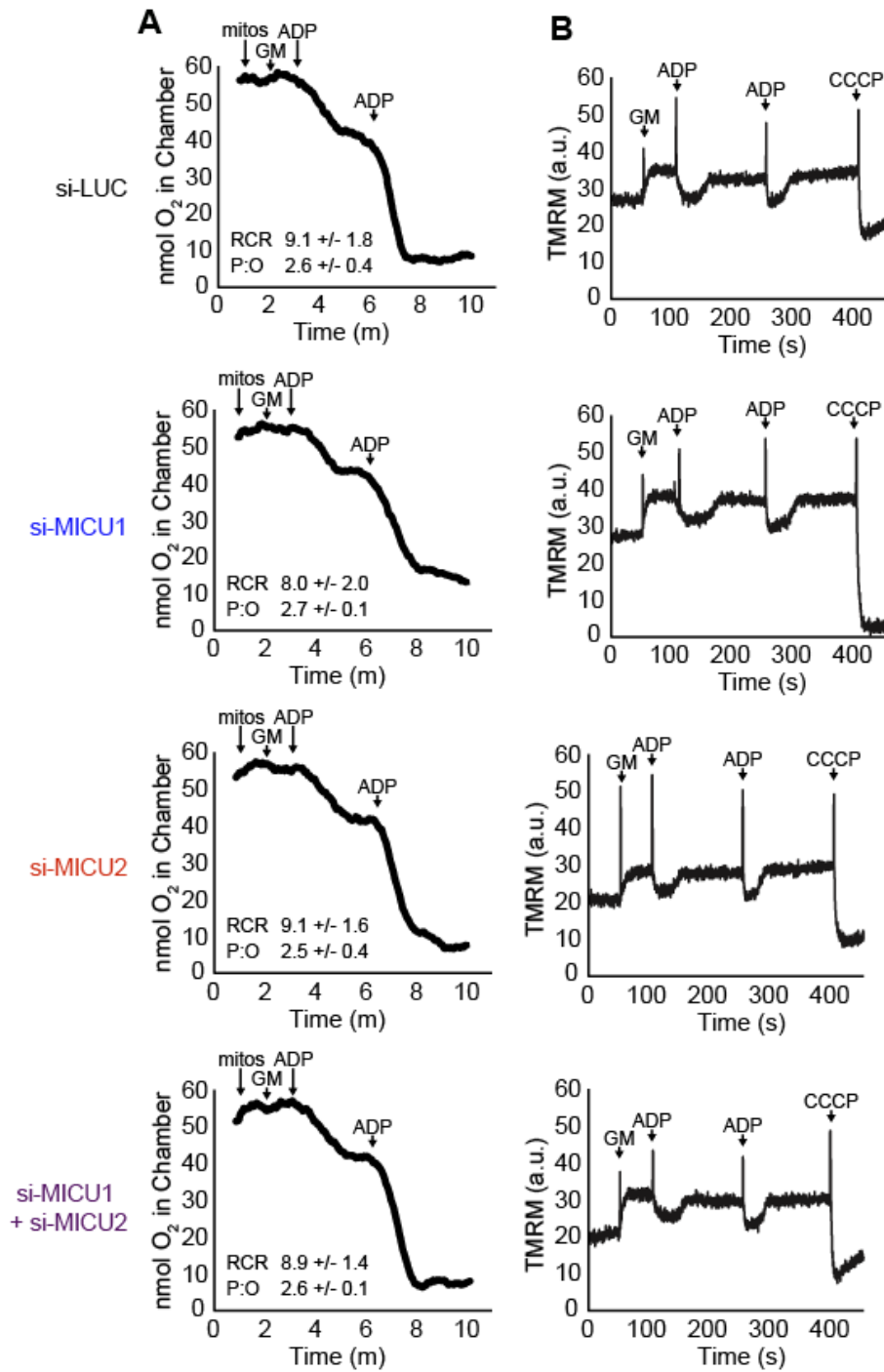


**Figure 4. Respiration and mitochondrial membrane potential are intact following *in vivo* silencing of *MICU1* and *MICU2* in mouse liver. (a)** Representative oxygen consumption traces measured in isolated mitochondria. Arrows denote addition of mitochondria, glutamate and malate (G/M), ADP and uncoupler (carbonyl cyanide m-chlorophenyl hydrazone, CCCP). Respiratory control ratios (RCR) and ADP:O ratios (P:O) were calculated from experiments performed on three separate mice per group. **(b)** Representative mitochondrial membrane potential traces measured in isolated mitochondria using tetramethyl rhodamine methyl ester (TMRM).

*In vivo silencing of MICU1 and MICU2 in mouse liver results in decreased mitochondrial calcium uptake.*

Next, I analyzed calcium uptake kinetics in mitochondria isolated from control and knockdown mice by adding a single spike of calcium to mitochondria suspended in buffer containing extramitochondrial Calcium Green-5N (CG5N) and observed the rate of calcium clearance by measuring CG5N fluorescence. Mitochondria from si-*MICU1* and si-*MICU2* mice demonstrated moderately impaired calcium uptake, whereas mitochondria from si-*MICU1* + si-*MICU2* mice demonstrated an additive defect (Figure 5a). This result was also observed when multiple spikes of calcium were added to mitochondria (Figure 5b). Interestingly, mitochondria from control and knockdown groups were able to clear the first spike of calcium, but differed significantly in their ability to clear a second pulse. This defect was additive in mitochondria from si-*MICU1* + si-*MICU2*, which demonstrated a near complete loss of buffering in response to the second calcium pulse. In addition, MCU protein expression was significantly decreased in knockdown mitochondria (Figure 5c). The degree of MCU protein loss correlated with the phenotype strength, raising the question of whether MCU loss was responsible for at least part of the observed phenotype. Similar to the effect of MICU2 knockdown in HeLa cells, loss of MICU2 resulted in significantly reduced MICU1 expression.

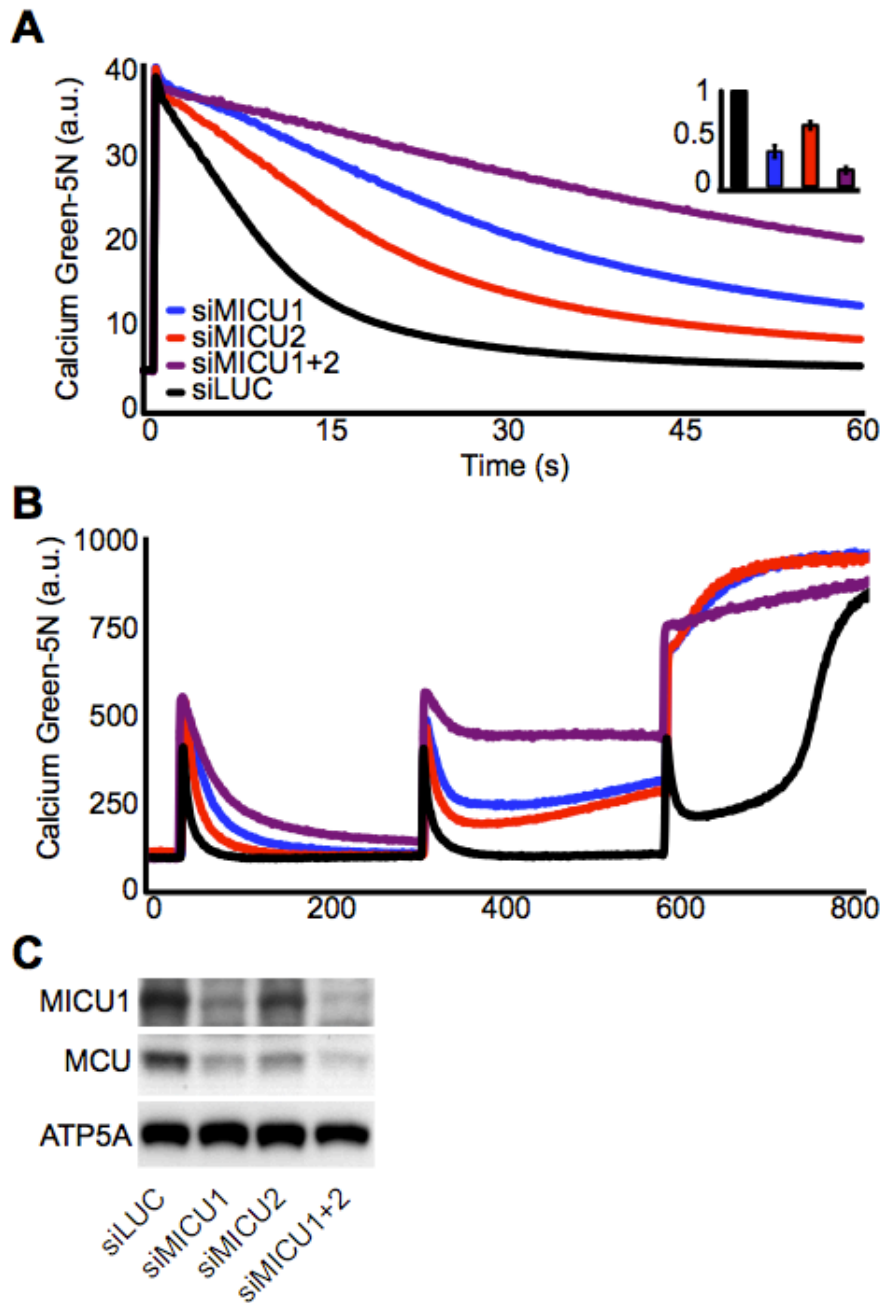


**Figure 5. Silencing MICU1 and MICU2 in mouse liver results in impaired calcium uptake.** (a) Calcium uptake in energized liver mitochondria following the addition of 50 mM  $\text{CaCl}_2$ . Inset reports linear fits of uptake between 5 and 10s normalized to si-*LUC* uptake. (b) Calcium uptake in energized liver mitochondria following the addition of multiple spikes of 50 mM  $\text{CaCl}_2$ . (c) Mouse liver mitochondria isolated from animals treated with si-*LUC*, si-*MICU1*, si-*MICU2* or si-*MICU1+2* were blotted with anti-*MICU1*, anti-*MCU* and control anti-*ATP5A*.

### *In vivo silencing of MICU1 and MICU2 alters MCU complex size*

Previous studies using blue native polyacrylamide gel electrophoresis (BN-PAGE) and western blot (WB) have demonstrated that a complex containing MCU is present at approximately 480 kDa. To gain insight into how silencing these proteins may affect the uniporter complex, I solubilized control and knockdown mitochondria in digitonin and performed BN-PAGE and western blot analysis. Blotting with anti-MCU revealed a shift in MCU complex size in knockdown mitochondria relative to si-LUC (Figure 6a). Interestingly, the degree of shift correlated with the severity of calcium uptake. This result was also observed in human cell lines stably expressing sh-*MICU1* and sh-LZ (Figure 6b). This could be rescued by introducing a cDNA encoding *MICU1* that was resistant to sh-RNA degradation, suggesting that this shift was specific to *MICU1* knockdown to rather than an off-target effect (Figure 6c).

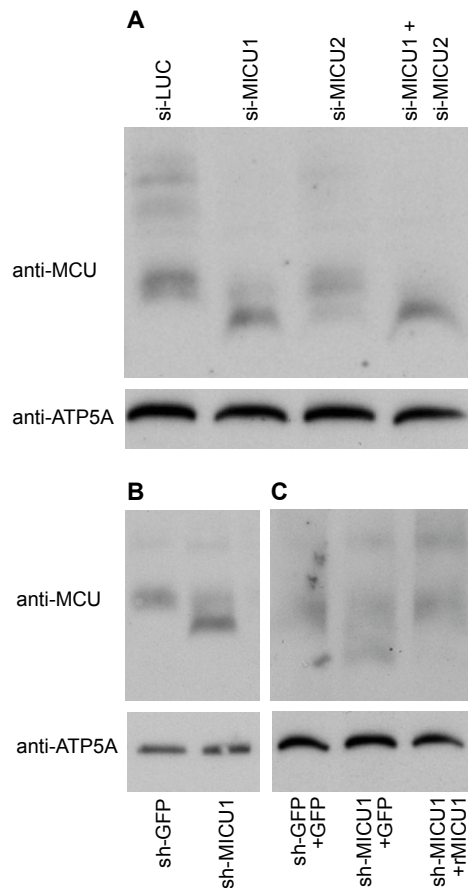


**Figure 6. Silencing MICU1 and MICU2 alters MCU complex size.** (a) BN-PAGE analysis of mouse liver mitochondria isolated from animals treated with si-LUC, si-MICU1, si-MICU2 or si-MICU1 and si-MICU2. Protein was transferred to a membrane and blotted for MCU and ATP5A (loading control). (b) BN-PAGE analysis of mitochondria isolated from HeLa cells stably expressing sh-GFP or sh-MICU1. Protein was transferred to a membrane and blotted for MCU and ATP5A (loading control). (c) BN-PAGE analysis of mitochondria isolated from HeLa cells stably expressing sh-GFP and GFP, sh-MICU1 and GFP or sh-MICU1 and rMICU1, a cDNA encoding MICU1 with eight synonymous mutations in the sh-MICU1 target sequence. MCU and ATP5A (loading control) were visualized by western blot.

*Stable expression of MICU2 rescues a calcium uptake defect in the setting of reduced MICU1*

The additive defect observed in simultaneous silencing of MICU1 and MICU2 in mouse liver suggests that they contribute independently to establishing the capacity of mitochondria to buffer calcium. However, the finding that their loss results in similar defects, including reduced calcium uptake and a shift in the MCU complex size,

indicates that they may have similar or overlapping roles in mediating mitochondrial calcium uptake. Although MICU1 knockdown results in a profound reduction in calcium uptake, it also significantly reduces MICU2 expression, which complicates the interpretation of this phenotype and raises the question of whether MICU2 can restore calcium uptake in the setting of reduced MICU1 expression.

To pursue this question, I stably expressed MICU2 in HeLa cells containing aequorin targeted to the mitochondrial matrix and introduced a sh-RNA targeting *MICU1*. Subsequently, I evaluated the ability of this cell line to transport calcium in response to histamine stimulation. This experiment revealed that MICU2 could restore mitochondrial calcium uptake in the setting of significantly reduced MICU1. Interestingly, although MCU expression was not decreased by loss of MICU1, it could not compensate for MICU1 loss. This strongly suggests that MICU2 specifically rescues a MICU1 phenotype either by stabilizing low levels of remaining MICU1 or directly compensating for MICU1 as a functional paralog.

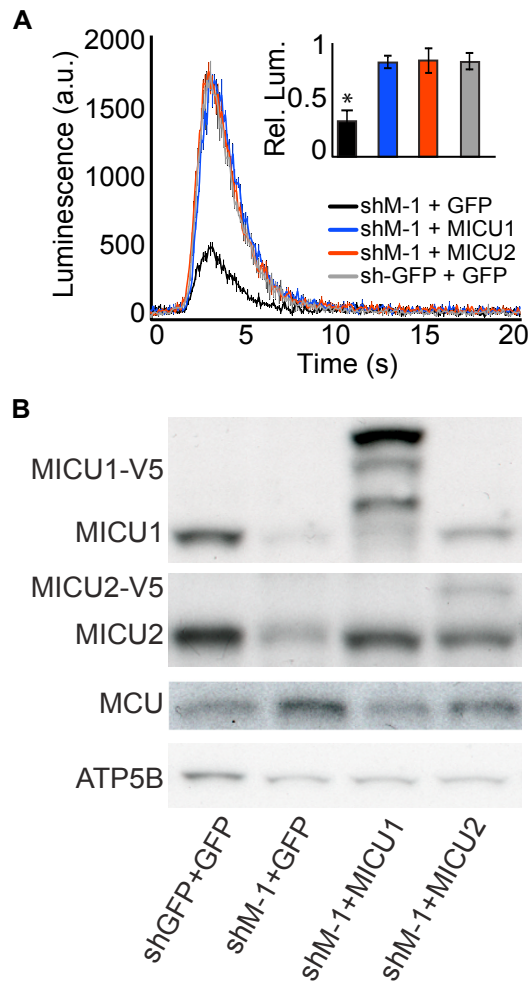


**Figure 7. Stable expression of MICU2 rescues a calcium uptake defect in the setting of reduced MICU1. (a)** Luminescence measurements of mitochondrial calcium following histamine stimulation in HeLa cells stably expressing aequorin targeted to the mitochondrial matrix (mean  $\pm$  s.e.m.,  $n = 4$ ). Inset reports statistics on the maximal luminescence (mean  $\pm$  s.d.,  $n = 8$ ,  $*P < 0.001$ ). **(b)** Western blot analysis of cells stably expressing sh-*MICU1* and *GFP*, sh-*MICU1* and *rMICU1*, sh-*MICU1* and *MICU2*, or sh-*GFP* and *GFP*.



## DISCUSSION

MICU1 represents the founding member of a family of paralogous proteins that includes MICU2 and MICU3, which likely arose by a gene duplication event prior to vertebrate evolution. Although both of these proteins have evidence as being mitochondrial, MICU2 is a high confidence mitochondrial-localized protein whereas MICU3 is likely mitochondrial but with lower confidence<sup>2</sup>. Therefore, MICU2 was prioritized for functional studies, but it is likely that MICU3 has a role in mitochondrial calcium uptake in a subset of tissues, notably in the neuromuscular system. In previous work, it was reported that loss of MICU1 in HeLa cells results in impaired mitochondrial calcium handling<sup>25</sup>, but it was unclear if this property extended to other cell types. The current study extends this finding to mouse liver, establishing the central role of MICU1 in regulating calcium transport in mammalian mitochondria. Our findings also demonstrate that silencing MICU1 or MICU2 *in vivo* in mouse liver results in moderately impaired mitochondrial calcium handling, whereas silencing both proteins has a more dramatic and perhaps additive effect.

In the present study, we demonstrate that MCU, MICU1 and MICU2 reside within a large complex, which we refer to as the uniporter complex. This is supported by results from immunoprecipitation studies and by the observation that these protein undergo cross-stabilization at the protein level across multiple cell types. Further supporting the notion that they reside in a complex, silencing of MICU1 or MICU2 results in a reduction in the MCU complex size as seen on BN-PAGE analysis. Taken together, these studies reveal that MICU2 is a bona fide member of the uniporter complex.

Though implicated in mitochondrial calcium handling, the exact molecular functions of MICU1 and MICU2 remain unclear. Mitochondria isolated from mouse liver in which MICU1 and MICU2 were silenced demonstrated a markedly impaired ability to clear large 50  $\mu$ M pulses of calcium. It is unclear if this is secondary to reduced MCU expression or a direct consequence of losing MICU1 and MICU2. At present, potential roles for MICU2 include 1) calcium sensing and regulation of MCU, 2) calcium buffering with a secondary impact on uniporter transport or 3) assembly and stabilization of MCU. Recent work suggests that MICU1 inhibits MCU at low cytosolic calcium concentrations, thereby setting the threshold for mitochondrial calcium uptake. In addition, there is compelling evidence that MICU1 senses calcium via its EF hands, which enable it to disinhibit MCU activity in response to appropriate spikes in cytosolic calcium. How MICU2 contributes to the regulation of MCU activity remains unclear.

An important question raised by our work is whether MICU1 and MICU2 have redundant or distinct molecular functions in mitochondrial calcium uptake. The evolutionary conservation of both paralogs in vertebrates, their distinct patterns of expression across organs and the presence of MICU1 and MICU2 in two different cell types point to complementary roles in cellular physiology. However, it is unclear if they are redundant or distinct on a molecular level. We attempted to complement a strong MICU1 phenotype in HeLa cells that we previously reported by expressing MICU2 on a MICU1 knockdown background. Although MICU2 was able to rescue this phenotype, we found that MICU2 also stabilized the protein expression of the small amount of MICU1, confounding the interpretation of this critical experiment. Resolving this question will likely require the use of a null genetic background in which the activity of one paralog can be rigorously assessed in the absence of the other paralog. Moving

forward, it will also be important to consider other mechanisms, including those involving MCUR1, LETM1 and NCLX that may additionally influence mitochondrial calcium physiology<sup>48-50</sup>.

Decades of research have shown that uniporter activity exists in all vertebrate tissues, but that its regulation is distinct<sup>16,40</sup>. It is possible that the relative expression of MICU1, MICU2 and MICU3 differ in a cell and state-specific manner to regulate uniporter activity. Under this model, multiple paralogs could be constitutively expressed in a single cell type, but variation in their relative abundance could give rise to functional differences in uniporter activity. If this model proves to be correct, it may enable the possibility of therapeutically targeting the uniporter in a tissue specific manner.

### **Acknowledgements**

- Designed, validated and produced mouse siRNA reagents: Roman Bogorad, Satya Kuchimanchi, Jack De Groot, Lauren Speciner, Nathan Taneja, Jonathan OShea, Victor Koteliansky; Alnylam Pharmaceuticals, Inc., Cambridge, Massachusetts, United States of America
- Assisted with mitochondrial isolation and assays: Yasemin Sancak, Kimberli J. Kamer, Laura Strittmatter

## Chapter 2: Developing a System for Proteoliposome Reconstitution of MCU

### INTRODUCTION

Targeting ion channels and transporters is a common mechanism of many therapeutic agents<sup>51</sup>. Drugs that alter the activity of plasma membrane channels and transporters include anesthetics, antiarrhythmic and antihypertensive agents. There are also compounds that act on intracellular channels and transporters to modulate cellular activity, including caffeine and dantrolene<sup>52,53</sup>. These drugs provide a precedent for targeting MCU, the channel-forming subunit of the mitochondrial calcium uniporter.

Although we showed that MCU is an essential component of the uniporter<sup>26</sup>, another group provided direct evidence that MCU is a calcium channel<sup>39</sup>. This group reconstituted purified MCU in planar lipid bilayers and obtained single channel recordings consistent with uniporter activity<sup>39</sup>. Their results appeared in a companion paper and complemented our *in vivo* results, which demonstrated that loss of MCU in mouse liver abolished calcium uptake. Together, these two bodies of work established MCU as the pore-forming subunit of the mitochondrial calcium uniporter.

Moving forward, we would like to establish a system for large-scale reconstitution of MCU in proteoliposomes. In this chapter, I describe my contributions to the three components of an *in vitro* reconstitution system including establishing an assay for transport, generating soluble protein, and incorporating it into vesicles. First, I discuss the development of a fluorescence-based liposome transport assay that will allow us to assess whether MCU proteoliposomes demonstrate biophysical properties consistent with the mitochondrial calcium uniporter. Subsequently, I will discuss preliminary work in generating soluble MCU for reconstitution into lipid vesicles. This system will allow us to confirm the results seen at the single-channel level and further explore the biophysical

properties of the mitochondrial calcium uniporter, which will enhance our understanding of mitochondrial calcium biology and motivate further experimental investigation. Ultimately, it may also provide a platform for a high-throughput *in vitro* chemical screen to identify novel therapeutics targeting mitochondrial calcium transport, which can then be validated in cell-based models.

## **MATERIALS AND METHODS**

### *Preparation of asolectin vesicles*

Asolectin lipid purchased from Avanti Polar Lipids (541601G) was dissolved in chloroform at a concentration of 25 mg/ml. It was mixed with an equal volume of buffer A (140 mM KCl, 10mM HEPES, pH 7.0) and 1 mM EGTA and incubated at 13°C for 24 hours. Buffer A was removed, and the asolectin chloroform solution was placed in a round-bottom flask and dried under a steady stream of nitrogen. The round-bottom flask was then placed in a dessicator overnight. The following day, asolectin was rehydrated in Buffer B (Buffer A + 50  $\mu$ M EGTA) to a final concentration of 35 mM. The solution was vortexed at high speed for 2 minutes and incubated at room temperature for at least 4 hours with a 2-minute vortexing period every hour. The rehydrated lipid was then sonicated for 2 minutes using a low-power sonicator. Calcium Green-5N (CG5N) was added to the rehydrated lipid to a final concentration of 84  $\mu$ M. The solution was taken through five freeze thaw cycles. The lipid was extruded 21 times using a 0.1  $\mu$ m filter. Following extrusion, the sample was diluted to 3 ml with Buffer B and poured over an equilibrated desalting column to remove unincorporated CG5N. The sample was then eluted in 3 ml of Buffer B for experimental analysis with a fluorescence spectrophotometer.

### *Measurement of calcium transport in asolectin vesicles*

The eluted sample was diluted in Buffer B to a final concentration of 0.2-2 mg/ml. Fluorescence (Ex. 506/Em. 531nm) was monitored at room temperature using a stopped flow spectrophotometer or a Perkin-Elmer LS-50B fluorescence spectrophotometer equipped with a stirring device. Calcium ionophore A23187 was

added at a concentration ranging from 500 nM to 5  $\mu$ M. This was followed by the addition of calcium (10 mM) or EGTA (1 mM). Experiments were performed in which the ionophore was added after the addition of calcium or EGTA. This scheme produced equivalent results.

#### *Cell-free expression of MCU*

MCU was cloned into a vector (pEXP5-CT/TOPO) optimized for cell-free expression. This vector was also selected because it has a C-terminal 6xHis tag for affinity purification and detection by western blot. MembraneMax Protein Expression Kit (A10632) was purchased from Invitrogen. Protein synthesis was carried out according to the directions outlined in the kit manual. *E. coli* extract, reaction buffer, amino acids and DNA were combined and incubated in a thermomixer (1200 rpm) at 37°C for 30 minutes. The reaction was then supplemented with feed buffer and amino acids and carried out for an additional two hours. Bacteriorhodopsin (bR) DNA was provided with the kit and used a positive control for protein expression.

#### *Analysis of MCU yield following cell-free expression*

To estimate total MCU production, protein was precipitated with acetone and the samples were analyzed using SDS-PAGE and western blot. To determine whether MCU was soluble, a portion of the reaction was spun at 20,000g for 30 minutes, and the supernatant was removed for acetone precipitation and western blot analysis. Quantitative estimates of total and soluble protein yield were made using a cocktail of five His-tagged proteins (Qiagen 34705) with known concentrations.

### *Supplementation of cell-free reactions with detergent or liposomes*

Cell-free reactions were supplemented with detergent at the beginning of the incubation period and the concentration was maintained for the duration of the reaction. Detergents and their concentrations were selected based on previous studies that tested the compatibility of detergents with cell-free expression systems<sup>54</sup>. Digitonin was purchased from Invitrogen, and DDM, Triton X-100, Brij-58, Brij-S20 and Brij-98 were purchased from Sigma. For reactions performed in the presence of liposomes, asolectin vesicles were added to the reaction mixture at concentrations ranging from 0.2 to 1 mg/ml.

### *Purification of MCU using nickel chromatography*

Spin columns containing nickel nitrilotriacetic acid (NTA) resin were purchased from Qiagen (31014) and used to purify soluble MCU from cell-free reactions supplemented with 1% digitonin or 0.2% Brij-98. The protocol outlined in the Qiagen manual for protein purification under native conditions from *E. coli* lysates was followed. Detergent concentrations used in the cell free reaction were maintained throughout the purification process. The flow-through, wash and elution fractions were collected, and protein was precipitated with acetone for SDS-PAGE and western blot analysis.

### *Analysis of cell-free MCU produced in the presence of liposomes*

Following the cell-free reaction, vesicles were purified by sucrose gradient centrifugation as previously described<sup>55</sup>. The reaction mixture was diluted with 25 mM HEPES-KOH to a final volume of 300  $\mu$ l and a final w/w sucrose concentration of 60%. This was placed at the bottom of a tube and a gradient was created using 56, 53, 50,



47, 44, 41, 38 and 36% sucrose solutions. The tubes were centrifuged for 40h at 280,000g at 10°C. Fractions were collected from the top, and protein from each fraction was precipitated using 10% trichloroacetic acid (TCA) for SDS-PAGE and western blot analysis. To assess protein insertion using a complementary method, vesicles were treated with urea following the cell free reaction<sup>55</sup>. This was achieved by recovering vesicles from the cell-free reaction by centrifugation at 24,000g for 10 minutes. The pellet was then resuspended in 200 µl of 20 mM Tris (pH 7.0) containing 4M urea. The vesicles were incubated for 30 minutes at room temperature. Subsequently, they were diluted 2x with 20 mM Tris containing 250 mM NaCl. The vesicles were then subjected to a high-speed spin at 285,000g for 30 minutes at 18 °C. The soluble and insoluble fractions were kept for SDS-PAGE and western blot analysis.

## RESULTS

### *Calcium transport can be measured in asolectin vesicles loaded with CG5N*

In this assay, lipid vesicles are loaded with a calcium indicator that fluoresces in the presence of calcium. A low affinity indicator was selected to reduce background signal due to low levels of calcium present in buffer and to ensure a robust response to calcium as it is transported into lipid vesicles. Calcium Green-5N (CG5N) has a  $K_D$  of  $\sim 14 \mu\text{M}$  (Invitrogen product manual), which is at least one order of magnitude greater than the majority of calcium indicators currently available. Therefore, it was chosen as the low-affinity indicator for this assay.

To establish a positive control for calcium transport, A23187, a bacterial calcium ion-carrier, was added to liposomes containing CG5N in the absence of calcium. Next, calcium was rapidly mixed with vesicles and fluorescence was monitored using a stopped flow spectrophotometer (Figure 1a). In the presence of A23187, robust calcium transport was detected in a dose-dependent manner that exceeded the slow increase in fluorescence due to calcium permeation through the vesicle membrane (Figure 1b). This proof-of principle experiment demonstrated that the vesicles were intact and that CG5N was a suitable indicator for measuring calcium transport in vesicles.

This assay was developed using phosphatidylcholine (22:1) (Avanti Polar Lipids), but once validated, was replaced with asolectin, a natural soybean extract containing a mixture of lipids, because numerous mitochondrial transporters have been reconstituted using this lipid, including LETM1, a  $\text{Ca}^{2+}:\text{2H}^+$  antiporter located on the inner membrane that contributes to calcium efflux from mitochondria<sup>49</sup>. Initially, the asolectin vesicles were tested using stopped flow spectrophotometry. Similar to liposomes containing phosphatidylcholine, these vesicles demonstrated a robust response to A23187.

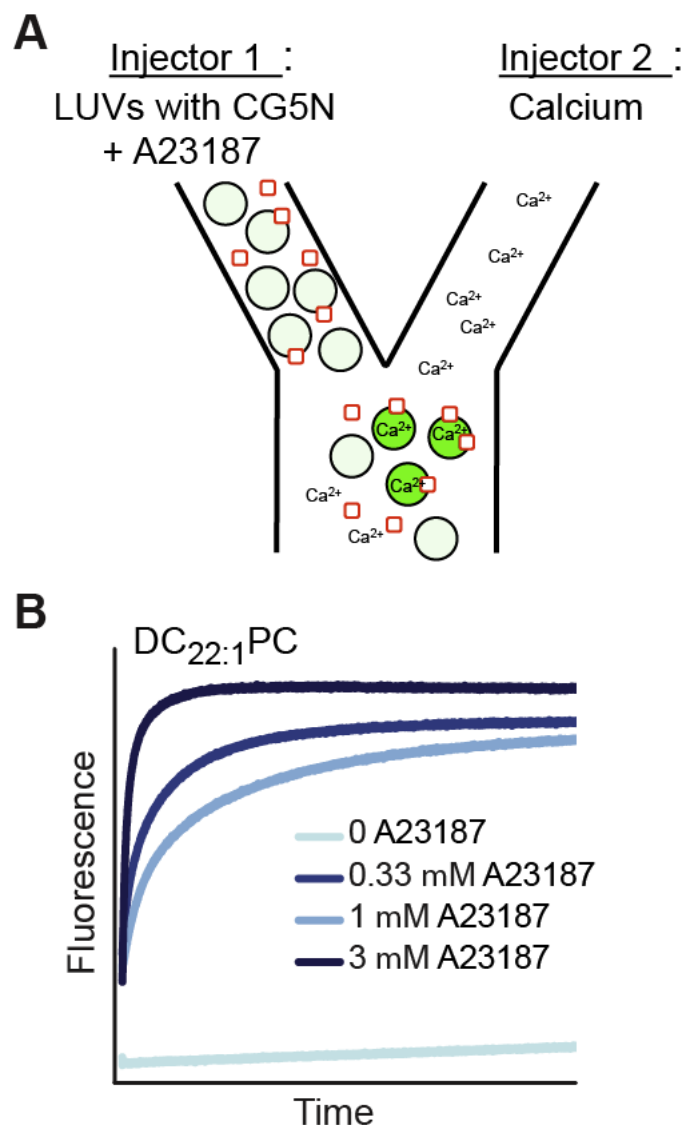


**Figure 1. Calcium transport in DC<sub>22:1</sub>PC liposomes loaded with CG5N.** (a) Schematic overview of the transport assay in a stopped flow spectrophotometer. (b) Dose-dependent calcium transport is detected in response to A23187.

After transport was validated in asolectin vesicles, the assay was established using a standard spectrophotometer. In this configuration, the vesicles were placed into a quartz cuvette and the excitation and emission wavelengths were set to match the spectral characteristics of CG5N, which undergoes an increase in emission intensity after binding micromolar amounts of calcium. In this assay, fluorescence was measured as a function of time, and A23187, calcium or EGTA was added at different time points

using a syringe. Although this approach lacks the kinetic resolution of the stopped flow method, it is sufficient to observe whether transport has occurred. In the future, this could be adapted to a plate reader format for high-throughput compound screening in which injectors coordinate the administration of calcium, EGTA and A23187 as a positive control.

In the initial set of experiments, the response of vesicles to A23187 was tested to find the minimal amount of vesicles needed to see a robust response. To start, liposomes were diluted to 2 mg/ml, and calcium (10mM) or EGTA (1mM) was added before a spike of 5  $\mu$ M A23187 was administered (Figure 2 a, b). As expected, influx was observed with calcium, and efflux was seen with EGTA, which established a concentration gradient across the liposome by chelating residual calcium present outside of the vesicles. Identical results were obtained if calcium or EGTA was added after the ionophore. To determine the minimal amount of liposomes required for the assay, serial dilutions were performed, which revealed that a robust response could be seen with 0.15 mg/ml of asolectin vesicles.

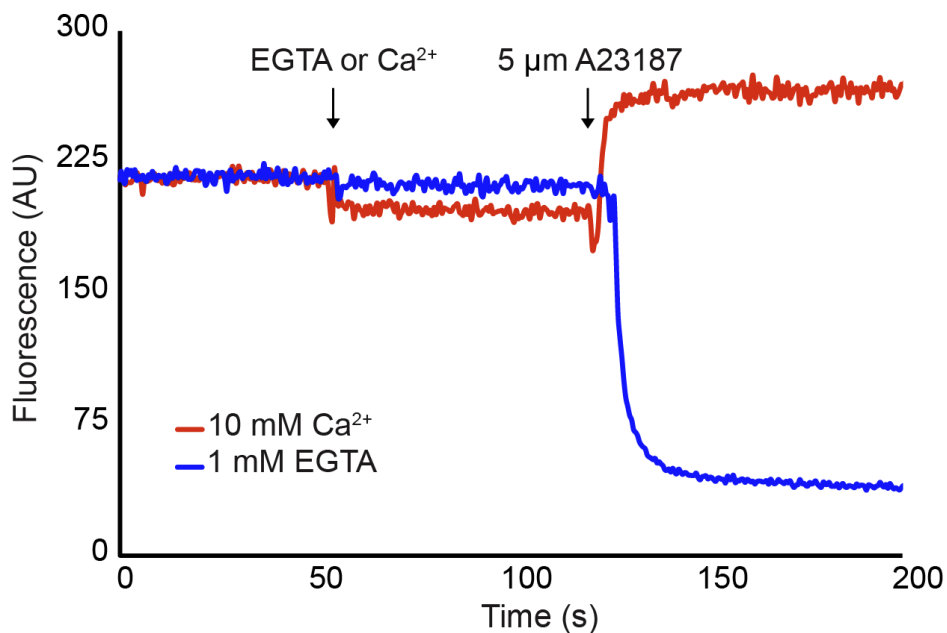


**Figure 2. Calcium transport in asolectin liposomes.** Liposomes were diluted to 2mg/ml and calcium transport was measured using a standard spectrophotometer.

Interestingly, the response to A23187 was substantially greater following the addition of EGTA compared to calcium. The signal decreased by approximately 5.5 fold after EGTA was added, whereas it increased by 0.35 fold following a spike of calcium. This was unexpected and may represent residual calcium in the buffer or contamination of asolectin lipid with high amounts of calcium. The results of these experiments indicate that an efflux assay in which EGTA is added to the buffer outside the liposomes may be preferable due to the substantial signal change in response to calcium efflux. In this configuration, if a transporter or channel is present, residual calcium within vesicles can exit due to a concentration gradient established by strong calcium chelator present outside the liposomes. Assuming unbiased insertion of protein into vesicles, an efflux assay should be equivalent to an influx assay for evaluating transport across proteoliposomes.

In July of 2011, I traveled to the laboratory of Dr. Andersen where I worked with post-doctoral fellow, Dr. Helgi Ingólfsson, to further optimize the stopped flow assay. Since the baseline signal of asolectin vesicles was unexpectedly high in my previous set of experiments performed on a standard spectrophotometer, I was interested in determining the maximum and minimum CG5N signal relative to baseline in the vesicles I prepared in this laboratory. To measure the maximum and minimum CG5N signal, the vesicles were lysed by treating them with 0.1% Triton or subjecting them to multiple freeze thaw cycles. This liberated the vesicle-encapsulated fluorophore, which was rapidly mixed with 10 mM CaCl<sub>2</sub> or 1 mM EGTA to determine the maximum and minimum CG5N signal (Figure 3 a, b).

Although these complementary methods gave consistent values for the minimum and maximum fluorescence, there was an unexpectedly slow response of liberated CG5N to calcium (Figure 3 a, b). This delayed response was also observed if CG5N was diluted in buffer, and calcium or EGTA was added. Since the kinetic rate constant for association of CG5N with calcium is on the order of microseconds, calcium should be able to bind and dissociate from CG5N within the dead time of the stopped flow machine, which is approximately 2 milliseconds<sup>56</sup>. This was an essential issue to resolve because in its current form, the assay did not distinguish free CG5N from transport into or out of liposomes.

Although puzzling, it was reasoned that this may reflect a contaminant metal in the fluorophore or in our buffer. For example, if CG5N binds to other metals with a low-affinity, their dissociation may be rate limiting, rather than calcium binding. To address this possibility, we decided to test whether the presence of metal chelators (e.g. EGTA) in our buffer can “strip” the fluorophore of contaminants to resolve this kinetic issue.

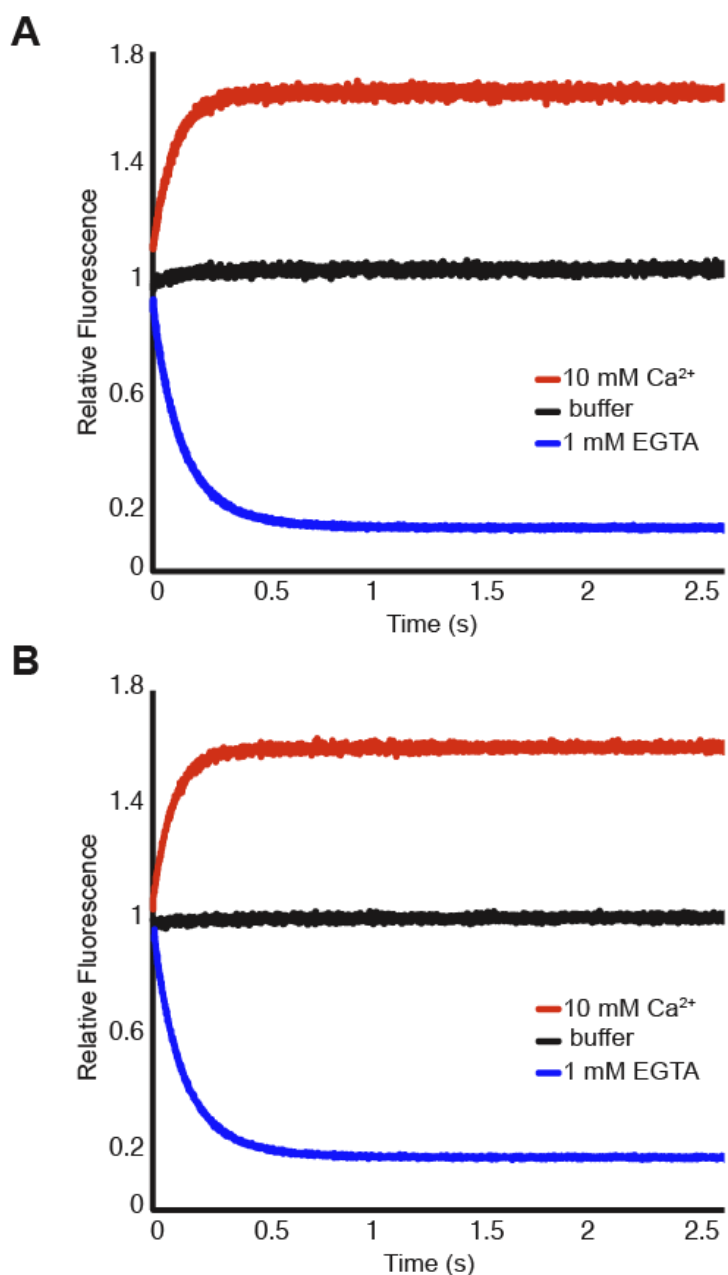


**Figure 3. Free CG5N demonstrates slow response kinetics to calcium and EGTA. (a)** Vesicles were lysed using 0.1% Triton and rapidly mixed with calcium, buffer or EGTA. **(b)** Vesicles were subjected to five freeze-thaw cycles to liberate encapsulated CG5N. Lysed vesicles were rapidly mixed with calcium, buffer or EGTA.

Therefore, our goal was to make vesicles in the presence of EGTA. We wanted to avoid adding excess EGTA because this could adversely affect vesicle integrity or chelate calcium that is transported across liposomes, blocking our ability to observe calcium transport. Thus, vesicles were lysed and an EGTA titration was performed to

find the minimum amount needed to “kill” the CG5N signal due to residual calcium, with the hope that this would also resolve the delayed kinetics observed when CG5N was released from lysed vesicles. This experiment revealed that 50  $\mu$ M EGTA was sufficient to minimize the CG5N signal.

To test whether the presence of EGTA within vesicles could prevent the delayed response of lysed vesicles to calcium, asolectin lipid was rehydrated in buffer containing 50  $\mu$ M EGTA, which was maintained throughout the entire vesicle preparation, including the freeze thaw cycles, extrusion and elution. Remarkably, this strategy was effective in resolving the delayed kinetics observed in the setting of lysed vesicles. When vesicles were lysed with 0.1% Triton (Figure 4a), the addition of calcium resulted in a stepwise jump in the fluorescent signal rather than a slower rise resembling true transport, as seen with the addition of A23187 (Figure 4b). Furthermore, the addition of EGTA reduced the baseline signal to its minimum value. This resulted in a ten-fold change in fluorescence following the addition of calcium (Figure 4b), which significantly improved the signal-to-noise ratio of the influx assay. Thus, the addition of EGTA to the vesicle preparation resolved multiple technical issues, including the inability to distinguish between lysed vesicles and rapid channel-mediated transport, and the small signal change seen in response to calcium influx.



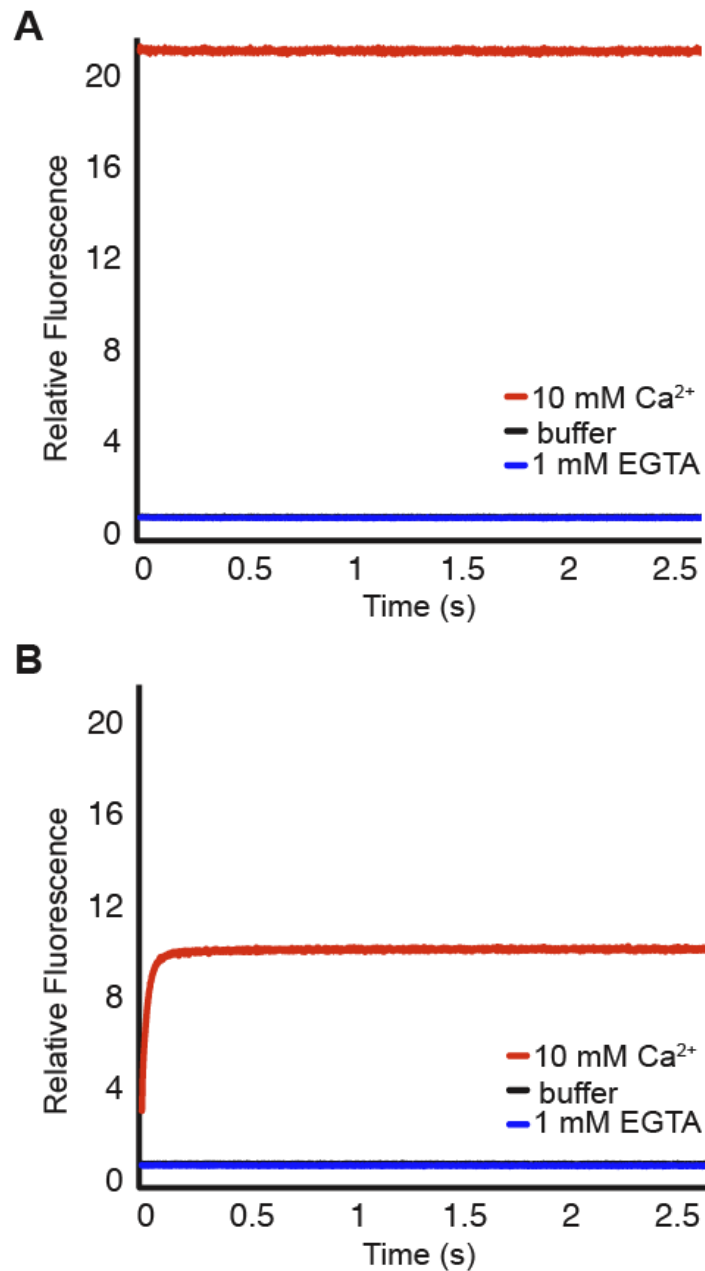


**Figure 4. Vesicles prepared with 50  $\mu\text{M}$  EGTA have normal response kinetics to calcium and EGTA. (a)** Vesicles were lysed using 0.1% Triton and rapidly mixed with calcium, buffer or EGTA. **(b)** Vesicles pre-mixed with A23187 were rapidly mixed with calcium, buffer or EGTA.

*MCU can be produced in a cell-free expression system*

In parallel to a collaborative effort in developing a liposome-based calcium transport assay, I also pursued a protocol for generating soluble MCU for proteoliposome reconstitution. Our first strategy was to express MCU in a cell-free

system using a commercially available kit for in vitro translation (IVT). Cell-free expression of membrane proteins for functional and structural studies represents an attractive alternative to recombinant expression in bacterial or yeast systems, which suffer from disadvantages such as protein aggregation, toxic effects on the host, and difficulty recovering intact protein from host cell membranes<sup>57,58</sup>. Traditionally, cell free reactions can be performed using bacterial or eukaryotic extracts to produce membrane proteins as a precipitate (P-CF) or in soluble form in the presence of detergent (D-CF) or lipid (L-CF)<sup>58</sup>.

MCU was cloned into a prokaryotic expression vector (pEXP5-CT/TOPO) containing a C-terminal 6xHis tag, which can be used for western blot analysis of protein yield and affinity purification. To generate protein, a commercially available kit from Invitrogen was ordered that utilizes *E. coli* extract and is optimized for expression of recombinant membrane proteins in microgram to milligram quantities. The kit also includes bacteriorhodopsin (bR) in pEXP5-CT/TOPO as a positive control for protein expression.

In initial experiments, MCU was partially insoluble following the CF reaction (Figure 5). Previous experiments have demonstrated that proteins produced in soluble form have a higher probability of being functional. Therefore, I decided to screen a set of detergents that could be added to the cell-free reaction to shift production of MCU into the soluble fraction.

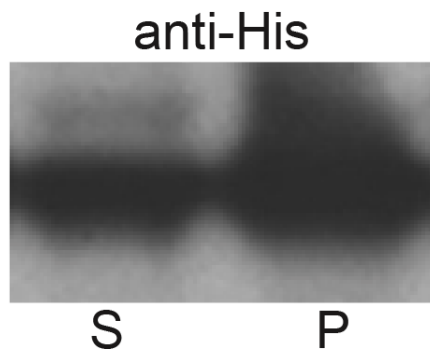


**Figure 5. MCU is partially insoluble following expression in a cell-free system.** Following IVT, the soluble (S) and insoluble (P) fractions were separated by centrifugation and analyzed by SDS-PAGE and western blot.

*A detergent screen identifies a set of detergents compatible with cell-free expression of soluble MCU*

A list of detergents was generated based on previous studies that tested detergents for their compatibility with cell-free systems<sup>54</sup>. Among the detergents tested include digitonin, DDM, Triton X-100, Brij-58, Brij-S20 and Brij-98. Each was tested at two concentrations based on values reported in previous studies in which cell-free reactions were supplemented with detergent. To assess the efficacy of each detergent, total protein production was compared to a reaction without detergent to ensure that the presence of the detergent did not adversely affect the reaction efficiency. In addition, the soluble and insoluble fractions were separated after the reaction by centrifugation and analyzed using SDS-PAGE and western blot. Figure 6 shows an example of this analysis in which three detergents were tested. As can be seen on the gel, 1% DDM and 1.5% Brij-58 result in a substantial amount of MCU in the insoluble fraction (Figure 6a). This is in contrast to 1% digitonin, which results in nearly 100% of MCU in the soluble fraction (Figure 6a). The results of the screen revealed that 1% digitonin and 0.2% Brij-98 are detergents compatible with CF production of soluble MICU3 (Figure 6b).

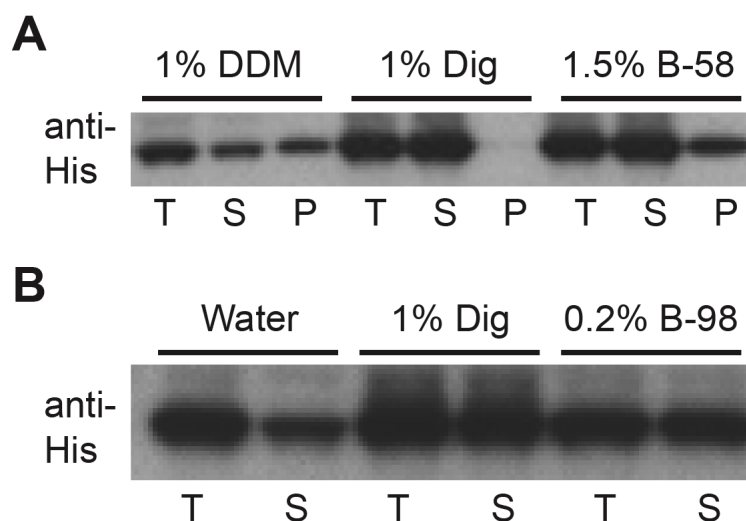


**Figure 6. A screen identifies two detergents that enable cell-free expression of soluble MCU.** (a) Results are shown from a subset of the detergents tested. Total (T), soluble (S) and insoluble (P) fractions are shown for each detergent. For reactions supplemented with 1% DDM and 1.5% Brig-58 (B-58), a fraction of MCU is insoluble. This is in contrast to reactions containing 1% digitonin (Dig) in which MCU is fully soluble. (b) Cell-free reactions supplemented with either 1% digitonin (Dig) or 0.2% Brij-98 (B-98) produce soluble MCU.

#### *Purification of soluble MCU using Ni-NTA spin columns*

Since the soluble fraction was contaminated by many proteins from the *E. coli* lysate, we were interested in developing a purification scheme prior to incorporating soluble MCU into lipid vesicles. We decided to use nickel affinity chromatography because MCU was synthesized with a C-terminal 6xHis tag. To choose the appropriate affinity system for purification, I needed an estimate of how much soluble MCU was produced by the cell-free system. Therefore, I performed serial dilutions of the soluble fraction and ran these on a gel with 5 6xHis-tagged protein standards with known concentrations. This enabled me to estimate the amount of soluble MCU generated by one 100  $\mu$ l cell-free reaction, which was between 10-50  $\mu$ g. Based on this, I chose to use Ni-NTA spin columns for affinity purification. Maintaining the detergent concentration through the entire purification, flow-through, wash and elution fractions were obtained. I took a sample from each fraction and precipitated the protein for SDS-PAGE and western blot

analysis. In the case of both detergents, the majority of the protein appeared in the elution fractions (Figure 7). Unfortunately, on a gel stained with coomassie brilliant blue R-250, soluble MCU was not the dominant band in the elution fraction, indicating the need for further purification or modifications to the cell-free reaction to boost yield.

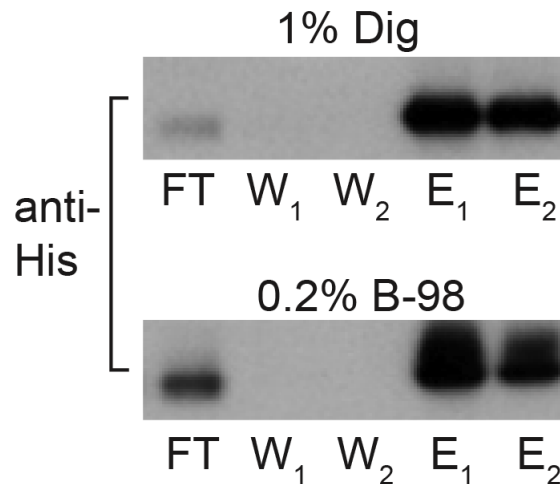


**Figure 7. Purification of soluble MCU using nickel affinity chromatography.** Cell-free reactions supplemented with 1% digitonin (Dig) or 0.2% Brij-98 (B-98) were processed using Ni-NTA spin columns. The flow-through (FT), wash (W<sub>1</sub> and W<sub>2</sub>) and elution (E<sub>1</sub> and E<sub>2</sub>) fractions were collected and analyzed using SDS-PAGE and western blot.

*MCU is associated with liposomes following cell-free expression supplemented with liposomes*

Since certain proteins are able to insert directly into liposomes during IVT, I also performed cell-free expression in the presence of pre-formed liposomes<sup>55,59,60</sup>. Based on previous studies<sup>55,59,60</sup>, I tested several liposome concentrations in the range of 0.2-2 mg/ml. After the reaction, I used two approaches to assess whether protein was associated with the vesicles. The first was sucrose gradient centrifugation, which was used to separate liposomes and any associated proteins from the rest of the cell-free extract<sup>55</sup>. This is a form of density gradient centrifugation, and it is an effective way to

separate liposomes from the rest of the reaction contents because are less dense and consequently float to the top. The cell-free reaction was diluted and a discontinuous sucrose gradient was layered on top of it. After spinning the tube at high speed for several hours, fractions were collected and analyzed by SDS-PAGE and western blot. In the reaction containing no liposomes, MCU was located in the bottom fractions (Figure 8). However, in the reaction containing 2 mg/ml of liposomes, the protein was found in middle and top fractions, indicating partial localization with liposomes (Figure 8).

To further assess whether MCU was associated with liposomes, I isolated the vesicles after the reaction using centrifugation, and resuspended them in urea to denature and remove loosely associated proteins<sup>55</sup>. Subsequently, the reaction was diluted and spun at high speed to pellet the liposomes. The supernatant (S2) and pellet (P) were saved for SDS-PAGE and western blot analysis, as was the supernatant resulting from the first centrifugation step in which the vesicles were isolated from the reaction mixture (S1). Interestingly, there was an enrichment of MCU in the pellet (P), suggesting that a substantial amount of MCU was associated or inserted into the liposomes. This was not seen when a control protein, CALM3, was taken through the cell-free reaction and urea treatment. In this case, CALM3 localized exclusively to the first supernatant (S1). Taken together, these two approaches provide evidence that a subset of MCU is associated or incorporated into liposomes. Unfortunately, when transport was tested in these vesicles, no increased calcium flux relative to control liposomes was observed. This could be due to a variety of factors, including insufficient yield, failure to insert or non-functional protein.

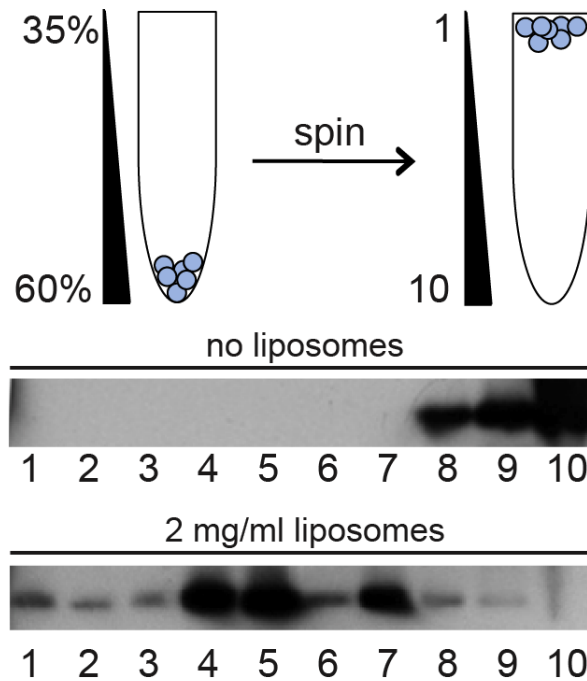


**Figure 8. Sucrose gradient centrifugation reveals that a subset of MCU is associated with liposomes following IVT. (a)** Schematic diagram depicting sucrose gradient centrifugation. **(b)** Following an extended high-speed spin, fractions were collected from the top of the tube and analyzed by SDS-PAGE and western blot using an anti-His antibody. In reactions supplemented with 2 mg/ml liposomes, there was a shift in the distribution of MCU toward the top, suggesting that some of the protein is associated with or inserted into liposomes.

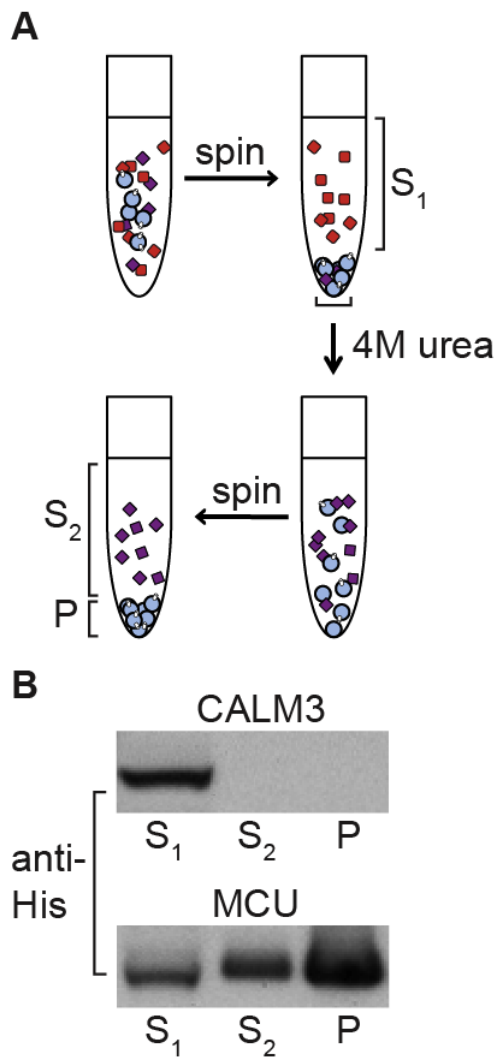


**Figure 9. MCU is associated with liposomes treated with 4M urea following IVT. (a)** Schematic diagram depicting the isolation of liposomes for urea treatment. **(b)** A subset of MCU was in the insoluble fraction (P) following urea treatment. A control protein (CALM3) was found exclusively in the soluble fraction isolated before urea treatment (S<sub>1</sub>).



## DISCUSSION

The development of a reconstitution system is an important next step for studying the biophysical properties of MCU and devising a platform for *in vitro* identification of compounds that target the mitochondrial calcium uniporter. In this chapter, I describe my contribution to the development of a liposome-based assay for calcium transport. I also discuss the application of a cell-free expression system for proteoliposome reconstitution of MCU. In the results section, I highlight two strategies for achieving reconstitution, which include production of detergent-solubilized protein and direct insertion of MCU into pre-formed liposomes. These approaches were devised based on previous studies in which cell-free expression systems were used to generate functional proteoliposomes.

At present, we have validated our liposome transport assay using A23187, a bacterial ionophore that binds calcium and facilitates transport across lipid membranes<sup>61</sup>. The addition of EGTA to the vesicle preparation has resolved two issues, including a delayed response of our fluorescent indicator to calcium and the high baseline fluorescent signal seen in asolectin vesicles due to residual calcium present in the buffer or lipid. As a result, we now have a sensitive influx assay that undergoes a several-fold change in signal intensity following calcium influx and distinguishes rapid channel-mediated transport from unstable vesicles that have release their encapsulated CG5N.

To generate protein for proteoliposomes, we decided to use a cell-free expression system rather than attempting recombinant expression in bacterial or yeast systems. The observation that proteins produced in soluble form have a higher probability of being functional motivated us to pursue this strategy because soluble

membrane proteins can be directly recovered from cell-free systems, particularly if reactions are supplemented with detergent or lipid<sup>58,62</sup>. This is in contrast to recombinant expression in bacteria or yeast where the vast majority of membrane proteins are recovered from insoluble inclusion bodies using detergents. Therefore, in order to avoid an insoluble intermediate, we conducted cell-free reactions in the presence of IVT-compatible detergents or pre-formed liposomes.

Our results revealed that soluble MCU could be generated by supplementing cell-free reactions with 1% digitonin or 0.2% Brij-98. Following the reaction, MCU was purified from the reaction mixture using Ni-NTA affinity chromatography. Although the majority of MCU appeared in the elution fraction, several other proteins were present in this fraction, as well. Furthermore, MCU was present in low abundance relative to these contaminant proteins, indicating the need for further optimization to boost protein yield. This may involve increasing reaction time or experimenting with different formulations, such as wheat germ extract. We will also explore the possibility of switching from a one-compartment batch reaction to a continuous-exchange system, which features two chambers separated by a semi-permeable membrane that allows for exchange of waste products and fresh, low-molecular weight substrates required for IVT, including amino acids and ATP<sup>58</sup>. Although more complex, continuous-exchange systems may represent a better alternative for producing high amounts of soluble protein.

In cell-free reactions supplemented with liposomes, a subset of MCU was associated with vesicles following cell-free expression. This was shown by two complementary approaches, including sucrose gradient centrifugation and treating liposomes with urea. Although more experiments are required to distinguish between strong association and insertion of MCU, and to assess whether contaminant proteins

are inserted into liposomes, these preliminary results indicate that direct insertion of MCU into pre-formed liposomes during IVT may be a viable strategy for generating proteoliposomes. As demonstrated by their response to A23187, the majority of vesicles were intact following cell-free expression. Unfortunately, we did not observe calcium transport in liposomes isolated from cell-free reactions in which MCU was produced, indicating reconstitution was not successful. This could be due to a variety of factors, including insufficient yield, failure to insert or non-functional protein.

Moving forward, we will focus on increasing protein yield in our cell-free expression system. This will provide more starting material for Ni-NTA affinity purification and allow us to explore complementary purification methods such as gel filtration. At the same time, it will increase the amount of MCU available for insertion into liposomes, which may enable us to detect transport in proteoliposomes isolated directly from the cell-free reaction. If we are unable to boost MCU production using cell-free expression, we will explore other systems, including recombinant expression in bacteria and yeast.

Once we generate a sufficient amount of soluble MCU, we will attempt to incorporate it into liposomes using a detergent-mediated strategy<sup>63</sup>. This approach involves partially solubilizing liposomes so that they are accessible to interact with soluble MCU. Following an incubation period, detergent will be removed using hydrophobic beads to induce the formation of vesicles containing lipid and protein, which can be monitored by an increase in side-scatter.

Naturally, this will present numerous challenges, including choosing a detergent, optimizing the protein-to-lipid ratio and finding a concentration of hydrophobic beads that removes detergent but leaves liposomes intact. In preliminary experiments, we

found that Triton X-100 solubilized liposomes and that it could be removed using hydrophobic beads to induce vesicle reformation. This suggests that Triton X-100 may be an attractive detergent choice for reconstitution, although its compatibility with soluble MCU needs to be tested in an experimental setting.

The prospect of reconstituting MCU is exciting. If we are able to demonstrate calcium transport activity, we will test whether it reflects previously reported biophysical and pharmacological properties of the uniporter, including high selectivity for calcium, sodium transport in divalent-free conditions and inhibition by Ru-360<sup>22</sup>. This system will enable us to further explore the biology of MCU by testing the effect of mutants on channel conductance, selectivity and response to Ru-360, which may motivate additional *in vivo* experiments. Furthermore, it will provide a platform for an *in vitro* chemical screen to identify compounds that alter MCU activity, which may represent novel therapies for human disease.

### **Acknowledgements**

- Assistance with technical design of transport assay: Helgi Ingolfsson, Olaf Andersen; Weill Cornell Medical College, New York, New York

## Conclusion

The recent molecular characterization of the mitochondrial calcium uniporter marks the end of a fifty search and opens a new era in molecular mitochondrial calcium biology. Now, there is a rich set of genetic approaches that can directly probe the role of mitochondrial calcium transport in cellular physiology and disease. In addition, the identification of MCU and MICU1 enables a diverse collection of biochemical and computational approaches to identify proteins that functionally interact with known components of the uniporter. Together, these studies will clarify the longstanding association of uniporter activity with cellular metabolism and apoptosis, as well as its relationship to the pathogenesis of numerous diseases, including neurodegeneration, cancer and ischemic injury.

In this thesis, I explore two areas within the growing field of mitochondrial calcium biology. First, I discuss the identification of MICU2, a previously uncharacterized protein important for mitochondrial calcium uptake. In this study, I define a family of paralogous proteins that include MICU1, MICU2 and MICU3, which likely arose by gene duplication event prior to vertebrate evolution, and present data that implicates both MICU1 and MICU2 in establishing the capacity of mitochondria to buffer calcium. Although more experiments are needed, our results suggest that MICU1 and MICU2 interact with MCU in the same cell type and that they have overlapping roles in mediating mitochondrial calcium buffering. Moving forward, it will be important to understand how these paralogous proteins partner with MCU to achieve high-capacity mitochondrial calcium uptake.

In a second body of work, I discuss my work in developing an *in vitro* system to characterize MCU, the pore-forming subunit of the mitochondrial calcium uniporter.

Although MCU demonstrated channel-activity in planar lipid bilayers, there are many unanswered questions regarding the biophysical properties of the uniporter, including its selectivity to other ions, allosteric activation by calcium and pharmacological response to a variety of compounds. In addition, it is not clear which residues contribute to calcium transport, the selectivity filter and response to Ru-360. Reconstitution of MCU in proteoliposomes will enable us to systematically address these questions using fluorescence spectroscopy and electrophysiology, which will further motivate *in vivo* studies. A scalable transport assay also opens up the possibility of performing an *in vitro* drug screen to identify compounds that target the uniporter, which may represent novel therapeutics for human disease.

As we learn more about the biology of mitochondrial calcium transport, we can design experiments to elucidate the role of this conserved pathway in cellular physiology and the pathogenesis of human disease. Although mutations in components of the respiratory chain cause a devastating class of disorders characterized by endocrine, neurological and muscle myopathies, it is unknown whether mutations in components of the uniporter give rise to inherited disorders. In addition, the association of defects in mitochondrial calcium transport with common pathologies such as cancer, neurodegeneration and ischemic injury has yet to be definitively proven. It is my hope that the work presented in this thesis will contribute to a deeper understanding of mitochondrial calcium biology, which will inform future studies exploring the role of mitochondrial calcium transport in human disease.

## Summary

Calcium signaling orchestrates a diverse set of cellular events, including muscle contraction, neurotransmission and growth<sup>64</sup>. The specific role of mitochondria in regulating cytosolic calcium is unclear at present, but there is evidence that they may play a critical role in decoding cytosolic calcium signals to initiate a cellular response<sup>8</sup>. The ability of mitochondria to transport large amounts of calcium was documented over fifty years ago<sup>14,15</sup>, but it was only recently that the first molecular components of the uniporter were identified<sup>25,26,39</sup>. These include MICU1, an EF-hand protein that may function as a regulatory component by sensing calcium, and MCU, the channel-forming subunit of the uniporter. Key to solving this mystery was an approach inspired by comparative physiology and integrative genomics.

Here, I discuss the identification of a previously uncharacterized regulator of mitochondrial calcium uptake that shares a common ancestor with MICU1. EFHA1, which we rename MICU2, physically interacts with MICU1 and MCU and undergoes coregulation with MICU1 at a protein level. Our physiology data suggest that MICU1 and MICU2 have independent contributions to establishing the capacity of mouse liver mitochondria to buffer calcium. In HeLa cells, MICU2 can rescue a defect in calcium uptake in the setting of reduced MICU1, whereas MCU cannot. This suggests that MICU2 either stabilizes low levels of MICU1 or directly compensates for MICU1 loss as a functional paralog. Future studies will elucidate how these proteins function as a complex to facilitate high-capacity calcium transport.

In addition, I describe my contribution to three components of an *in vitro* system for proteoliposome reconstitution of MCU, the channel-forming subunit of the mitochondrial calcium uniporter. These include developing an assay for transport,

expressing soluble protein and incorporating it into vesicles. At present, we have established a robust transport assay and are currently exploring ways to generate soluble protein for incorporation into lipid vesicles. The development of a reconstitution system will enable detailed biophysical analysis of the uniporter, which will complement ongoing *in vivo* studies. Furthermore, it may provide a platform for *in vitro* identification of compounds that modulate mitochondrial calcium transport.



## References

1. Andersson, S.G. *et al.* The genome sequence of *Rickettsia prowazekii* and the origin of mitochondria. *Nature* **396**, 133-40 (1998).
2. Pagliarini, D.J. *et al.* A mitochondrial protein compendium elucidates complex I disease biology. *Cell* **134**, 112-23 (2008).
3. Mitchell, P. Coupling of phosphorylation to electron and hydrogen transfer by a chemi-osmotic type of mechanism. *Nature* **191**, 144-8 (1961).
4. Kennedy, E.P. & Lehninger, A.L. Oxidation of fatty acids and tricarboxylic acid cycle intermediates by isolated rat liver mitochondria. *The Journal of biological chemistry* **179**, 957-72 (1949).
5. Sano, S., Inoue, S., Tanabe, Y., Sumiya, C. & Koike, S. Significance of mitochondria for porphyrin and heme biosynthesis. *Science* **129**, 275-6 (1959).
6. Brownie, A.C., Grant, J.K. & Davidson, D.W. The in vitro enzymic hydroxylation of steroid hormones. II. Enzymic 11 beta-hydroxylation of progesterone by ox-adrenocortical mitochondria. *The Biochemical journal* **58**, 218-25 (1954).
7. Danial, N.N. & Korsmeyer, S.J. Cell death: critical control points. *Cell* **116**, 205-19 (2004).
8. Hajnoczky, G., Robb-Gaspers, L.D., Seitz, M.B. & Thomas, A.P. Decoding of cytosolic calcium oscillations in the mitochondria. *Cell* **82**, 415-24 (1995).
9. Jouaville, L.S., Ichas, F., Holmuhamedov, E.L., Camacho, P. & Lechleiter, J.D. Synchronization of calcium waves by mitochondrial substrates in *Xenopus laevis* oocytes. *Nature* **377**, 438-41 (1995).
10. Kaftan, E.J., Xu, T., Abercrombie, R.F. & Hille, B. Mitochondria shape hormonally induced cytoplasmic calcium oscillations and modulate exocytosis. *The Journal of biological chemistry* **275**, 25465-70 (2000).
11. Denton, R.M. & McCormack, J.G. The role of calcium in the regulation of mitochondrial metabolism. *Biochemical Society transactions* **8**, 266-8 (1980).
12. Balaban, R.S. The role of Ca(2+) signaling in the coordination of mitochondrial ATP production with cardiac work. *Biochim Biophys Acta* **1787**, 1334-41 (2009).
13. Szalai, G., Krishnamurthy, R. & Hajnoczky, G. Apoptosis driven by IP(3)-linked mitochondrial calcium signals. *The EMBO journal* **18**, 6349-61 (1999).
14. Deluca, H.F. & Engstrom, G.W. Calcium uptake by rat kidney mitochondria. *Proc Natl Acad Sci U S A* **47**, 1744-50 (1961).
15. Vasington, F.D. & Murphy, J.V. Ca ion uptake by rat kidney mitochondria and its dependence on respiration and phosphorylation. *J Biol Chem* **237**, 2670-7 (1962).
16. Carafoli, E. & Lehninger, A.L. A survey of the interaction of calcium ions with mitochondria from different tissues and species. *Biochem J* **122**, 681-90 (1971).
17. Igbavboa, U. & Pfeiffer, D.R. EGTA inhibits reverse uniport-dependent Ca<sup>2+</sup> release from uncoupled mitochondria. Possible regulation of the Ca<sup>2+</sup> uniporter by a Ca<sup>2+</sup> binding site on the cytoplasmic side of the inner membrane. *J Biol Chem* **263**, 1405-12 (1988).
18. Moore, C.L. Specific inhibition of mitochondrial Ca<sup>++</sup> transport by ruthenium red. *Biochem Biophys Res Commun* **42**, 298-305 (1971).
19. Rossi, C., Azzi, A. & Azzone, G.F. Ion transport in liver mitochondria. I. Metabolism-independent Ca<sup>++</sup> binding and H<sup>+</sup> release. *The Journal of biological chemistry* **242**, 951-7 (1967).

20. Selwyn, M.J., Dawson, A.P. & Dunnett, S.J. Calcium transport in mitochondria. *FEBS letters* **10**, 1-5 (1970).
21. Rizzuto, R., Simpson, A.W., Brini, M. & Pozzan, T. Rapid changes of mitochondrial Ca<sup>2+</sup> revealed by specifically targeted recombinant aequorin. *Nature* **358**, 325-7 (1992).
22. Kirichok, Y., Krapivinsky, G. & Clapham, D.E. The mitochondrial calcium uniporter is a highly selective ion channel. *Nature* **427**, 360-4 (2004).
23. Mironova, G.D. *et al.* Isolation and properties of Ca<sup>2+</sup>-transporting glycoprotein and peptide from beef heart mitochondria. *J Bioenerg Biomembr* **14**, 213-25 (1982).
24. Zazueta, C., Zafra, G., Vera, G., Sanchez, C. & Chavez, E. Advances in the purification of the mitochondrial Ca<sup>2+</sup> uniporter using the labeled inhibitor 103Ru360. *J Bioenerg Biomembr* **30**, 489-98 (1998).
25. Perocchi, F. *et al.* MICU1 encodes a mitochondrial EF hand protein required for Ca(2+) uptake. *Nature* **467**, 291-6 (2010).
26. Baughman, J.M. *et al.* Integrative genomics identifies MCU as an essential component of the mitochondrial calcium uniporter. *Nature* **476**, 341-5 (2011).
27. Csordas, G. *et al.* MICU1 controls both the threshold and cooperative activation of the mitochondrial Ca(2+)(+) uniporter. *Cell Metab* **17**, 976-87 (2013).
28. Mallilankaraman, K. *et al.* MICU1 is an essential gatekeeper for MCU-mediated mitochondrial Ca(2+) uptake that regulates cell survival. *Cell* **151**, 630-44 (2012).
29. de la Fuente, S., Matesanz-Isabel, J., Fonteriz, R.I., Montero, M. & Alvarez, J. Dynamics of mitochondrial Ca<sup>2+</sup> uptake in MICU1-knockdown cells. *Biochem J* (2013).
30. Chaudhuri, D., Sancak, Y., Mootha, V.K. & Clapham, D.E. MCU encodes the pore conducting mitochondrial calcium currents. *Elife* **2**, e00704 (2013).
31. Raffaello, A. *et al.* The mitochondrial calcium uniporter is a multimer that can include a dominant-negative pore-forming subunit. *EMBO J* **32**, 2362-76 (2013).
32. Sancak, Y. *et al.* EMRE is an essential component of the mitochondrial calcium uniporter complex. *Science* **342**, 1379-82 (2013).
33. Racay, P. *et al.* Mitochondrial calcium transport and mitochondrial dysfunction after global brain ischemia in rat hippocampus. *Neurochemical research* **34**, 1469-78 (2009).
34. Murphy, A.N., Bredesen, D.E., Cortopassi, G., Wang, E. & Fiskum, G. Bcl-2 potentiates the maximal calcium uptake capacity of neural cell mitochondria. *Proceedings of the National Academy of Sciences of the United States of America* **93**, 9893-8 (1996).
35. Tang, T.S. *et al.* Disturbed Ca<sup>2+</sup> signaling and apoptosis of medium spiny neurons in Huntington's disease. *Proceedings of the National Academy of Sciences of the United States of America* **102**, 2602-7 (2005).
36. Cousse, E. *et al.* G37R SOD1 mutant alters mitochondrial complex I activity, Ca(2+) uptake and ATP production. *Cell Calcium* **49**, 217-25 (2011).
37. Logan, C.V. *et al.* Loss-of-function mutations in MICU1 cause a brain and muscle disorder linked to primary alterations in mitochondrial calcium signaling. *Nat Genet* (2013).
38. Pan, X. *et al.* The physiological role of mitochondrial calcium revealed by mice lacking the mitochondrial calcium uniporter. *Nat Cell Biol* **15**, 1464-72 (2013).

39. De Stefani, D., Raffaello, A., Teardo, E., Szabo, I. & Rizzuto, R. A forty-kilodalton protein of the inner membrane is the mitochondrial calcium uniporter. *Nature* **476**, 336-40 (2011).
40. Sparagna, G.C., Gunter, K.K., Sheu, S.S. & Gunter, T.E. Mitochondrial calcium uptake from physiological-type pulses of calcium. A description of the rapid uptake mode. *The Journal of biological chemistry* **270**, 27510-5 (1995).
41. Frank-Kamenetsky, M. *et al.* Therapeutic RNAi targeting PCSK9 acutely lowers plasma cholesterol in rodents and LDL cholesterol in nonhuman primates. *Proceedings of the National Academy of Sciences of the United States of America* **105**, 11915-20 (2008).
42. Akinc, A. *et al.* A combinatorial library of lipid-like materials for delivery of RNAi therapeutics. *Nature biotechnology* **26**, 561-9 (2008).
43. Akinc, A. *et al.* Targeted delivery of RNAi therapeutics with endogenous and exogenous ligand-based mechanisms. *Molecular therapy : the journal of the American Society of Gene Therapy* **18**, 1357-64 (2010).
44. Semple, S.C. *et al.* Rational design of cationic lipids for siRNA delivery. *Nature biotechnology* **28**, 172-6 (2010).
45. Gohil, V.M. *et al.* Nutrient-sensitized screening for drugs that shift energy metabolism from mitochondrial respiration to glycolysis. *Nat Biotechnol* **28**, 249-55 (2010).
46. Moffat, J. *et al.* A lentiviral RNAi library for human and mouse genes applied to an arrayed viral high-content screen. *Cell* **124**, 1283-98 (2006).
47. Brini, M., Pinton, P., Pozzan, T. & Rizzuto, R. Targeted recombinant aequorins: tools for monitoring [Ca<sup>2+</sup>] in the various compartments of a living cell. *Microscopy research and technique* **46**, 380-9 (1999).
48. Mallilankaraman, K. *et al.* MCUR1 is an essential component of mitochondrial Ca<sup>2+</sup> uptake that regulates cellular metabolism. *Nat Cell Biol* **14**, 1336-43 (2012).
49. Jiang, D., Zhao, L. & Clapham, D.E. Genome-wide RNAi screen identifies Letm1 as a mitochondrial Ca<sup>2+</sup>/H<sup>+</sup> antiporter. *Science* **326**, 144-7 (2009).
50. Hajnoczky, G. & Csordas, G. Calcium signalling: fishing out molecules of mitochondrial calcium transport. *Curr Biol* **20**, R888-91 (2010).
51. Overington, J.P., Al-Lazikani, B. & Hopkins, A.L. How many drug targets are there? *Nat Rev Drug Discov* **5**, 993-6 (2006).
52. Ehrlich, B.E., Kaftan, E., Bezprozvannaya, S. & Bezprozvanny, I. The pharmacology of intracellular Ca(2+)-release channels. *Trends Pharmacol Sci* **15**, 145-9 (1994).
53. Ozawa, T. Effects of FK506 on ca release channels (review). *Perspect Medicin Chem* **2**, 51-5 (2008).
54. Klammt, C. *et al.* Evaluation of detergents for the soluble expression of alpha-helical and beta-barrel-type integral membrane proteins by a preparative scale individual cell-free expression system. *FEBS J* **272**, 6024-38 (2005).
55. Berrier, C. *et al.* Coupled cell-free synthesis and lipid vesicle insertion of a functional oligomeric channel MscL MscL does not need the insertase YidC for insertion in vitro. *Biochimica et biophysica acta* **1808**, 41-6 (2011).
56. Naraghi, M. T-jump study of calcium binding kinetics of calcium chelators. *Cell Calcium* **22**, 255-68 (1997).
57. Grisshammer, R. Understanding recombinant expression of membrane proteins. *Curr Opin Biotechnol* **17**, 337-40 (2006).

58. Schwarz, D., Dotsch, V. & Bernhard, F. Production of membrane proteins using cell-free expression systems. *Proteomics* **8**, 3933-46 (2008).
59. Hovijitra, N.T., Wu, J.J., Peaker, B. & Swartz, J.R. Cell-free synthesis of functional aquaporin Z in synthetic liposomes. *Biotechnol Bioeng* **104**, 40-9 (2009).
60. Varnier, A. *et al.* A simple method for the reconstitution of membrane proteins into giant unilamellar vesicles. *The Journal of membrane biology* **233**, 85-92 (2010).
61. Balasubramanian, S.V., Sikdar, S.K. & Easwaran, K.R. Bilayers containing calcium ionophore A23187 form channels. *Biochem Biophys Res Commun* **189**, 1038-42 (1992).
62. Klammt, C. *et al.* Cell-free expression as an emerging technique for the large scale production of integral membrane protein. *FEBS J* **273**, 4141-53 (2006).
63. Rigaud, J.L. & Levy, D. Reconstitution of membrane proteins into liposomes. *Methods Enzymol* **372**, 65-86 (2003).
64. Clapham, D.E. Calcium signaling. *Cell* **131**, 1047-58 (2007).